A genome-wide Approximate Bayesian Computation approach suggests only limited numbers of soft sweeps in humans over the last 100,000 years

Guillaume Laval, Etienne Patin, Pierre Boutillier, Lluis Quintana-Murci

1   **A genome-wide Approximate Bayesian Computation approach suggests only limited**

2   **numbers of soft sweeps in humans over the last 100,000 years**

3

4

5

6   Guillaume Laval[1,2,3,*], Etienne Patin[1,2,3], Pierre Boutillier[5] and Lluis Quintana-Murci[1,2,3,4]

7

8   [1]Human Evolutionary Genetics, Institut Pasteur, 75015 Paris, France

9   [2]Centre National de la Recherche Scientifique, UMR2000, 75015 Paris, France

10   [3]Center of Bioinformatics, Biostatistics and Integrative Biology, Institut Pasteur, 75015 Paris,

11   France

12   [4]Human Genomics and Evolution, Collège de France, 75005 Paris, France

13   [5]Department of Systems Biology, Harvard Medical School, Boston, Massachusetts 02115,

14   USA.

15

16

17   *Correspondence: glaval@pasteur.fr

18

1   Over the last 100,000 years, humans have spread across the globe and encountered a

2   highly diverse set of environments to which they have had to adapt. Genome-wide scans

3   of selection are powerful to detect selective sweeps. However, because of unknown

4   fractions of undetected sweeps and false discoveries, the numbers of detected sweeps

5   often poorly reflect actual numbers of selective sweeps in populations. The thousands of

6   soft sweeps on standing variation recently evidenced in humans have also been

7   interpreted as a majority of mis-classified neutral regions. In such a context, the extent

8   of human adaptation remains little understood. We present a new rationale to estimate

9   these actual numbers of sweeps expected over the last 100,000 years (denoted by X) from

10   genome-wide population data, both considering hard sweeps and selective sweeps on

11   standing variation. We implemented an approximate Bayesian computation framework

12   and showed, based on computer simulations, that such a method can properly estimate

13   X. We then jointly estimated the number of selective sweeps, their mean intensity and

14   age in several 1000G African, European and Asian populations. Our estimations of X,

15   found weakly sensitive to demographic misspecifications, revealed very limited numbers

16   of sweeps regardless the frequency of the selected alleles at the onset of selection and the

17   completion of sweeps. We estimated ~80 sweeps in average across fifteen 1000G

18   populations when assuming incomplete sweeps only and ~140 selective sweeps in non-

19   African populations when incorporating complete sweeps in our simulations. The

20   method proposed may help to address controversies on the number of selective sweeps

21   in populations, guiding further genome-wide investigations of recent positive selection.

Introduction

Evaluating the legacy of positive, Darwinian selection in the human genome has proved crucial for identifying the genes underlying the broad morphological and physiological diversity observed across human populations, and for increasing our understanding of the genetic architecture of adaptive phenotypes. Genome-wide scans for positive selection have been largely guided by the selective sweep model (Hernandez, et al. 2011), a model in which advantageous mutations increase in frequency until fixation under the pressure of positive selection (Maynard Smith and Haigh 1974), see (Pritchard, et al. 2010) for a review. These studies have provided a flurry of candidate loci, e.g., (Voight, et al. 2006; Frazer, et al. 2007; Sabeti, et al. 2007; Tang, et al. 2007; Williamson, et al. 2007; Pickrell, et al. 2009b; Grossman, et al. 2010; Granka, et al. 2012; Grossman, et al. 2013; Fagny, et al. 2014; Pybus, et al. 2015; Schrider and Kern 2017), see .(Vitti, et al. 2013; Jeong and Di Rienzo 2014; Fan, et al. 2016) for reviews.

There is a little overlap across different genome-wide studies and false discovery rates remain high (Teshima, et al. 2006; Akey 2009; Hsieh, et al. 2016). Nevertheless, the lowest empirical P-values (P-values computed from genome-wide observed data) tend to remain significant after the computation of P-values from neutral computer simulations (Hsieh, et al. 2016), suggesting that top candidates usually put forward in genome-wide scans contain a fraction of true positives. The top candidates detected in the 1000 Genomes (1000G) CEU population (Auton, et al. 2015) using simulated P-values contain ~5 genomic regions with selection signals found significant after correction for the high numbers of tests performed genome-wide (-log(P-value)>8) (Grossman, et al. 2013). Unfortunately, it is fairly well-known that such multiple testing corrections applied to discard false positives also discard true targets of selection, because increasing detection thresholds also reduce the statistical power to detect sweeps (Pavlidis and Alachiotis 2017).

1   Recently, simulation-based machine learning algorithms implemented to detect selective

2   sweeps (Pybus, et al. 2015; Schrider and Kern 2016, 2017) and classify them into hard or soft

3   sweeps, revealed up to ~1,000 soft sweeps in non-African 1000G populations (Schrider and

4   Kern 2017). The hard sweeps refer to sweeps on *de novo* advantageous mutations (frequency

5   equal to $1/2N$ at the onset of selection) (Maynard Smith and Haigh 1974; Hermisson and

6   Pennings 2005). In contrast, the soft sweep model as investigated by (Schrider and Kern

7   2017) refers to selective sweeps on standing variation as defined in (Hermisson and Pennings

8   2005), i.e. mutations at frequency higher than $1/2N$ at the onset of selection (Orr and

9   Betancourt 2001; Innan and Kim 2004; Hermisson and Pennings 2005; Przeworski, et al.

10   2005; Pennings and Hermisson 2006a).

11   However, Harris and colleagues (2018) argued that these high numbers of soft sweeps

12   can be predicted on the basis of the error rates observed when classifying neutral sites,

13   highlighting a spurious inflation of the numbers of detected soft sweeps due to false positives

14   (see (Harris, et al. 2018) for details). This recent debate illustrates the lack of *ad-hoc* methods

15   that formally estimate actual numbers of selective sweeps in populations (e.g., numbers of

16   sweeps occurred over a given time span). Genome-wide scans for selection are designed to

17   detect sweeps but the numbers of detected/classified sites, e.g., (Li and Stephan 2006; Pybus,

18   et al. 2015; Schrider and Kern 2017), poorly estimate the actual numbers of sweeps because

19   of the burden of false positives. When using weakly or moderately stringent detection

20   thresholds, the lists of detected sweeps are potentially enriched in false positives (the majority

21   of detected sweeps can be neutral regions with spurious signal of selection). Therefore, as

22   mentioned above, in genome-wide studies we are forced to apply stringent detection

23   thresholds to discard these false positives. This may drastically reduce the number of detected

24   sweeps (see the ~862 and ~18 sweeps on average retained with the default and a most

25   stringent probability threshold of 0.9 used in the machine learning classifier (Schrider and

4

1   Kern 2017; Harris, et al. 2018)). These reduced numbers are likely far from being

2   representative of all true targets of selection. Indeed, many true targets of selection cannot be

3   detected because of a diminished statistical power when applying stringent thresholds,

4   resulting in an unknown fraction of false negatives, e.g., sweeps of weak intensity (weak

5   selection coefficients or very recent ages of selection) already hardly detectable even at

6   nominal thresholds of $P<0.01$. As a consequence, despite the high number of genome-wide

7   selection scans performed and the development of sophisticated methods, the numbers of loci

8   truly under positive selection in populations and, therefore, the contribution of positive

9   selection to recent human adaptation remain poorly understood, from rare numbers of classic

10 sweeps (Pritchard, et al. 2010; Hernandez, et al. 2011) to high numbers of soft sweeps

11 (Schrider and Kern 2017).

12   Overall, current methods are therefore related to numbers of detected sweeps not to

13 actual numbers of selective sweeps in populations, which can markedly differ because of

14 reasons described above (statistical power and detection thresholds). In this manuscript, we

15 present a simulation-based method that directly estimates these actual numbers of selective

16 sweeps in populations, denoted by X for the rest of the study. We did not attempt to detect

17 sweeps separately. We rather considered X as a parameter in a model of the genome-wide

18 effects of positive selection. To estimate X, we implemented an approximate Bayesian

19 computation (ABC) method (Beaumont, et al. 2002) based on summary statistics that

20 summarize the genome-wide signals of selection and correlate with X, as shown below by

21 computer simulations (see the results section). The ABC method presented here does not

22 output a list of detected sweeps but can help to design and/or interpret normal genome-wide

23 scans by providing general indications about the numbers of sweeps really expected in the

24 analyzed populations (scripts and software are available on demand).

5

1   We applied this method to several African, European and Asian 1000G populations

2   (Online Methods, Supplementary Table S1). In particular, we aimed to show the suitability of

3   our approach in the context of the high numbers of sweeps previously found, by considering

4   hard and soft sweep models as investigated by Schrider and Kern (Schrider and Kern 2017).

5   We thus considered selection models whereby advantageous mutations exhibit a non-zero

6   selection coefficient s since a specific time t. We considered t ranged from present to 3,500

7   generations ago (the last 100,000 years assuming a generation time of 28 years (Fenner 2005;

8   Moorjani, et al. 2016)}) and frequency of the selected allele when the sweep begins, denoted

9   by p_{start}, ranged from $1/2N$ (hard sweeps) to 0.2. This corresponds to the same soft sweep

10   scenario as investigated by Schrider and Kern (Schrider and Kern 2017), who ignored the soft

11   sweep scenario that considers multiple independent advantageous mutations at a single locus

12   (Garud, et al. 2015). Note that our simulation-based method can easily be updated in order to

13   also incorporate soft sweeps on multiple advantageous mutations. Finally, we considered

14   lower selection coefficient values, i.e., s ranged from 0.001 to 0.05, and avoided using flat

15   distributions as previously done (Schrider and Kern 2017). We rather randomly drawn s from

16   distributions enriched in low values as expected (e.g., ~60% of mutations were predicted

17   nearly neutral or with a moderate effect on fitness, i.e., with $s \leq 1\%$ (Boyko, et al. 2008)).

18   We jointly estimated X and the numbers of sweeps with very low ($1/2N \leq p_{start} < 0.01$), low

19   ($0.01 \leq p_{start} < 0.1$) and intermediate ($0.1 \leq p_{start} < 0.2$) initial frequencies of the selected alleles,

20   denoted by X_1, X_2 and X_3 respectively (in our model $X = X_1 + X_2 + X_3$). We did not estimate

21   the number of hard sweeps *stricto senso* ($p_{start} = 1//2N$) as classically performed (Schrider and

22   Kern 2017). Instead, we merged hard and soft sweeps with very low p_{start} into the same

23   category X_1 because such sweeps left genomic signatures virtually indistinguishable (see

24   (Jensen 2014) for a review). For example, the probability to misclassify soft sweeps as hard

25   sweeps increases when the initial frequency of the selected allele approaches $1/2N$ (Peter, et

6

1   al. 2012) since at such low frequency these two scenario generate similar signals of selection

2   (Przeworski, et al. 2005; Ferrer-Admetlla, et al. 2014; Jensen 2014). Finally, we jointly

3   estimated the Xs (X, X_1, X_2 and X_3) and the average intensity and age of selection, $S =$

4   $1/X \sum_1^X s_i$ and $T = 1/X \sum_1^X t_i$, with s_i and t_i being the intensity and age of the ith selective

5   sweep.

6

Results

Overview of the ABC Approach

9   For the clarity of the manuscript, we present in this section an overview of the rational and

10   methods implemented in our ABC approach.

11   ABC approaches are based on simulated data that mimic the empirical data to analyze

12   and on statistics that both summarize each dataset and exhibit a monotonic relationship with

13   the parameter to estimate. Here we simulated whole-genome sequence (WGS) data that mimic

14   the 1000G data, i.e., ~3Gb of DNA sequences for about 100 individuals sampled per

15   population. We used summary statistics based on the widely used comparison between neutral

16   mutations, labelled here ENVs (Evolutionary Neutral Variants), and mutations potentially

17   targeted by selection, labelled PSV (Possibly Selected Variants), e.g., synonymous and non-

18   synonymous comparison (Kimura 1977; Mcdonald and Kreitman 1991). Our rational was

19   motivated by previous studies showing that positive selection causes genome-wide excesses

20   of candidate SNPs of selection (i.e., those with extreme values for a given neutrality statistic)

21   within or nearby genes relative to intergenic regions (e.g., coding SNPs or *cis*-acting eQTLs

22   *vs* intergenic SNPs (Voight, et al. 2006; Frazer, et al. 2007; Barreiro, et al. 2008; Kudaravalli,

23   et al. 2009; Jin, et al. 2012; Fagny, et al. 2014; Schmidt, et al. 2019)). In such studies, the

24   ENV SNP class is the neutral baseline used to control for false discoveries (similar rates of

25   false positive are expected across SNP classes (Barreiro, et al. 2008)). As summary statistic,

1   we used the odds ratio for selection (OR) (Kudaravalli, et al. 2009), which assesses this

2   genome-wide excess of candidate SNPs in PSVs relative to ENVs using all candidate SNPs

3   treated equally regardless of their individual *P*-values. The OR being approximately a ratio

4   between the percentages of candidate SNPs in PSVs and ENV, this summary statistic is thus

5   expected close to one under neutrality and above one under selection (Kudaravalli, et al.

6   2009; Fagny, et al. 2014). Based on computer simulations, we show in the next section that

7   the OR exhibits a monotonic relationship with *X*.

8   The ENVs are easy to conceptualize. In real data, they are intergenic SNPs at some

9   distance from the nearest gene and purged from any functional sites to be unaffected by

10   selection. In contrast, the PSVs contains all potential targets of selection and neutral nearby

11   SNPs (Supplementary Fig. S1). For example, in real data the PSVs correspond to

12   nonsynonymous mutations and their neighbors (e.g., synonymous and intronic mutations) or

13   regulatory mutations and their neighbors (e.g., variants located upstream/downstream of genes

14   or in remote regulatory regions). We need to incorporate in PSVs these nearby SNPs in order

15   to take into account the hitchhiking effects of positive selection. Indeed, selective sweeps

16   produce clusters of candidate SNPs in the vicinity of the targets of selection whereas under

17   neutrality candidate SNPs are more uniformly scattered (Voight, et al. 2006). The magnitude

18   of such clustering depends on the intensity and age of selection and thus provides information

19   for our estimations of *X*, *S* and *T*. In simulations, the PSVs are randomly defined (the

20   remaining mutations are ENVs) and contain *X* selective sweeps of various intensity, age and

21   frequency of the selected alleles at the onset of selection (each PSV region does not contained

22   a target of selection but all simulated targets of selection are defined as PSVs).

23   The desired ABC posterior distributions are computed in each 1000G population by

24   comparing simulated and empirical WGS datasets each summarized by a vector of *K* ORs, *K*

25   being the number of neutrality statistic used. Because background selection (BGS) may

1   generate spurious positive selection signatures (Coop, Pickrell, Novembre, et al. 2009;

2   Pritchard, et al. 2010; Hernandez, et al. 2011), we decided to focus on neutrality statistics

3   previously found insensitive to BGS (Zeng, et al. 2006; Fagny, et al. 2014), i.e., Fay and Wu's

4   *H* (F&W-*H*) (Fay and Wu 2000), iHS (Voight, et al. 2006), DIND (Barreiro, et al. 2009),

5   ΔiHH (Grossman, et al. 2010), and XP-EHH (Sabeti, et al. 2007). Overall, the posterior

6   distributions obtained are the parameter values underlying the simulated ORs that best fit with

7   the empirical 1000G ORs. We use posterior mean as point estimate and the 95% credible

8   intervals (CI) boundaries to assess the uncertainty of the estimations.

9

10   **Odds Ratio for selection reflects the number of selective sweeps**

11   To test the unknown relationships between X and the OR for selection, we simulated WGS

12   data with different fixed numbers of selective sweeps, $X = [0, 50, 100, 150]$ (Online

13   Methods). The simulated WGS were obtained using recombination profiles randomly drawn

14   from human recombination maps (Frazer, et al. 2007) and a demographic model previously

15   inferred, as classically done (Peter, et al. 2012; Grossman, et al. 2013; Nakagome, et al. 2016;

16   Schrider and Kern 2017; Smith, et al. 2018; Uricchio, et al. 2019) (Online Methods). Because

17   we aimed to gain information by incorporating inter-population statistics such as the XP-

18   EHH, we did not use one-population models, as used by Schrider and Kern (Schrider and

19   Kern 2017). Instead, we used a three-populations demographic model calibrated to replicate

20   the allele frequency spectrum, population subdivision and linkage disequilibrium in the YRI

21   (Africa), CEU (Europe) and CHB (Asia) populations (Schaffner, et al. 2005; Grossman, et al.

22   2010; Grossman, et al. 2013) and used by (Grossman, et al. 2013; Pybus, et al. 2015) to detect

23   selective sweeps in the 1000G populations. Specifically, to simulate the X selective sweeps in

24   one population we assumed neutrality (X=0) in the two other populations, e.g., to simulate X

25   sweeps in Africa (YRI) we jointly simulated the European (CEU) and Asian (CHB)

9

1 populations as two neutral references populations. We incorporated the X selected regions

2 within simulated neutral DNA sequences to form ~3Gb of WGS in which the randomly

3 defined ENVs and PSVs respectively cover 30% and 70% of the genome (these proportions

4 corresponds to the proportions used to analyze the 1000G populations, see below). Finally, for

5 each neutrality statistic used we defined candidate SNPs (top 1% of SNPs) (Online Methods)

6 and we computed the ORs (Online Methods) separately for the F&W-H, iHS, DIND, ΔiHH,

7 and for two XP-EHHs (we obtained a total of 6 ORs since in a three-populations branching

8 model, as the one used in this study, there are two XP-EHH per population).

9   To simulate X sweeps per WGS data (Online Methods), p_{start} was randomly drawn from

10 the allele frequency spectrum at the generation t excluding values higher than 0.2 in

11 agreement with (Schrider and Kern 2017). The s and t parameters were randomly drawn from

12 flat distributions, $s \sim U(0.001, 0.05)$ and $t \sim U(0, 100) \, kya$, and we excluded complete

13 sweeps (sweeps at fixation) using a rejection algorithm. By excluding complete sweeps, we

14 reproduced in our simulations the excess of mutations with low or moderate effect on fitness

15 previously evidenced (Boyko, et al. 2008). Indeed, the resulting distributions of s (and also t)

16 really used for our simulations are enriched in low values (Fig. 1A), since (all other things

17 being equal) complete sweeps tend to be stronger (or older) than incomplete sweeps.

18 However, we started our analysis by excluding complete sweeps because previous results

19 support limited numbers of complete sweeps in humans, e.g., lack of extreme differences in

20 allele frequency between populations due to fixation events (Coop, Pickrell, Kudaravalli, et

21 al. 2009; Pritchard, et al. 2010; Hernandez, et al. 2011). This data-driven assumption was

22 further relaxed by considering both complete and incomplete sweeps in our simulations (see

23 the sections below).

24   We observed a monotonic relationship between X and the ORs, i.e., the six ORs increase

25 with X in every simulated scenario (Fig. 1B, supplementary Fig. S2). As expected, the values

1 of ORs depend on the frequencies of advantageous alleles at the onset of selection

2 (supplementary Fig. S2). The lowest ORs were obtained when simulating sweeps with initial

3 frequencies of the advantageous alleles, p_{start}, ranged from 0.01 to 0.2. Indeed, soft sweeps

4 typically have weaker effects on linked sites (Przeworski, et al. 2005; Pennings and

5 Hermisson 2006b; Pritchard, et al. 2010), resulting in a low enrichment of candidate SNPs in

6 the vicinity of the targets of selection. The highest simulated ORs were obtained for hard

7 sweeps *stricto senso* ($p_{start}=1/2N$) and soft sweeps with very low initial frequencies

8 ($1/N{\leq}p_{start}<0.01$). In addition, simulated ORs obtained for these two scenario were found to be

9 very similar, as expected (Przeworski, et al. 2005; Peter, et al. 2012; Ferrer-Admetlla, et al.

10 2014; Jensen 2014). This observation confirms that hard sweeps and soft sweeps on very rare

11 standing variation are almost indistinguishable on the basis of their outcomes (supplementary

12 Fig. S2), which justifies the merging of these two scenarios. In the following, we do not

13 provide separate estimates of the numbers of hard sweeps and only provide estimations of

14 numbers of sweeps on very rare standing variants as a whole ($p_{start}<1\%$, X_1).

15

16 **Odds Ratio for selection are poorly sensitive to demographic assumptions.**

17 As expected, the ORs values follow the power to detect selection as previously assessed for

18 iHS and XP-EHH assuming various demographic histories (highest, intermediate and lowest

19 power in the African, European and Asian demography respectively (Pickrell, et al. 2009b)).

20 For example, the European and Asians ORs found lower than in Africa (Fig. 1B) reflect a

21 lower enrichment of candidate SNPs, in agreement with the reduced power to detect selection

22 in bottlenecked populations relative to expanding populations (Pickrell, et al. 2009a; Huff, et

23 al. 2010; Gunther and Schmid 2011; Grossman, et al. 2013; Fagny, et al. 2014). Interestingly,

24 only little difference in the behavior of ORs was observed across populations simulated with

25 contrasting demographic histories (i.e., African expansions *vs* Eurasian bottlenecks, Fig. 1B).

1   Moreover, the Asian and European simulated ORs are virtual identical albeit slightly lower in

2   Asia (e.g., 2.3 *vs* 2.4 in average for iHS with X=100, Fig. 1B) whereas the Asian bottleneck is

3   four times stronger than in Europe. These observations suggest that the subsequent ABC

4   estimations of X will be weakly affected by potential demographic misspecifications (this

5   specific point is tested in the next sections below). Taken together, our results show that the

6   OR for selection contain information on X (monotonic relationship, see above) without being

7   largely affected by demography, which supports the use of such a summary statistic in an

8   ABC framework.

9

10   **Accuracy of the ABC estimations**

11   The ABC method was implemented using simulations identical to those presented in Fig. 1,

12   except that X was randomly drawn in flat prior distributions, $X \sim U(0, 200)$ (Online

13   Methods), opposed to fixed values (priors used for s and t are enriched in low values because

14   we excluded complete sweeps, see Fig. 1A). To assess the accuracy of the estimations (Fig. 2)

15   we simulated new WGSs following the same recombination and demographic model and

16   treated them as empirical data for which the parameter values are known (Online Methods).

17   We found unbiased estimations of X when simulating African, European or Asian

18   demography (Fig. 2A), as shown by the linear correlations observed between ABC estimates

19   and their corresponding true values (Fig. 2B). Such ABC estimates can thus be compared

20   between populations since they are not biased by specific demographic events, such as the

21   strong bottlenecks experienced by the non-African populations. We found a similar accuracy

22   for the estimations of X_1 (1/2N≤p_{start}<0.01), X_2 (0.01≤p_{start}<0.1) and X_3 (0.1≤p_{start}<0.2) (Fig.

23   2B). We also estimated S and T in all the demographic scenario simulated (Supplementary

24   Figs. S3-5) but found a diminished accuracy with respect to the estimations of X (e.g.,

25   underestimations and overestimations of S and T respectively when the selection is strong and

1   recent in average, Supplementary Figs. S3-4). (As an internal control of the method, the CIs

2   consistently predicted the range of values within which the true parameters were found

3   (Supplementary Figs. S6-7, see also the 90% COV in Fig. 2B and Supplementary Figs. S3-4).

4   These results show that six ORs used in combination may successfully estimate X, with

5   low or moderate credible intervals relative to the simulated priors (Supplementary Fig. S6).

6   By analogy with normal genome-wide scans, our estimations of X seem to be weakly

7   sensitive to false negative and positive signals. False positives do not contribute to ORs

8   thanks to the use of ENVs as an internal neutral control, as illustrated by the estimations of X

9   close to 0 under neutrality (Fig 2A) due to ORs fluctuating around one (i.e., similar rates of

10   candidate SNPs across ENV and PSV classes, Fig 1B). In contrast, every selected region with

11   more than 1% of candidate SNPs positively contributes to the OR proportionally to its

12   intrinsic rate of candidate SNPs: selected regions with much more than 1% of candidate SNPs

13   (e.g., true positives after multiple testing correction) contribute a lot and those with rates

14   moderately higher than 1% (e.g., false negatives undetected after Bonferroni correction) also

15   contribute but to a lesser extent. Moreover, thanks to the simulation of parameters that drive

16   the statistical power to detect sweeps in normal selection scans (e.g., intensity of selection,

17   demography), the model also predicts the expected fraction of sweeps with rates of candidate

18   SNPs slightly below neutral thresholds (e.g., false negatives that cannot even be detected at

19   unadjusted thresholds). Altogether, our estimations are not upward biased by neutral regions

20   exhibiting spurious signatures of selection and also include a large fraction of sweeps that

21   would not be detected by normal genome-wide scans (no systematic underestimation of X,

22   Fig. 2).

23   However, these results have been obtained under a perfectly known demography while in

24   real life, the demography is only partially known. Because our method, like every model-

25   based method, should be affected by incorrect assumptions which may bias the estimations,

1   we carefully tested the effect of demographic misspecifications on the estimations of X

2   obtained in each 1000G population (see the next sections below).

3

4   **Limited numbers of incomplete selective sweeps in the 1000G populations**

5   In this first round of estimations we assumed complete sweeps only. We thus analyzed 15

6   African, European and Asian 1000G populations separately (five populations per continent,

7   Supplementary Table S1) using priors and simulations shown in Figs. 1A and 2B (the prior

8   distribution used for s reproduces the expected enrichment of mutations with low or moderate

9   effect on fitness (Boyko, et al. 2008)). As in simulations and for each population in which X

10   was estimated, the two reference populations used to compute the interpopulation statistics

11   were of differing continental origin, and were chosen from the populations previously used to

12   calibrate the demographic model used (YRI, CEU or CHB) (Grossman, et al. 2010;

13   Grossman, et al. 2013). Based on the VEP annotation of the 1000G data, we defined PSVs as

14   all SNPs located within genic regions, including regions annotated as upstream and

15   downstream which often contain regulatory elements, as well as any presumed regulatory

16   sites located in intergenic regions (Supplementary Fig. S8, Online Methods). As already

17   mentioned, variants neighboring functional mutations need to be included in PSVs to account

18   for the clustering of candidate SNPs around putative targets of selection (Supplementary Fig.

19   S1). Under this definition, PSVs account for ~70% of the genome-wide variation (~30% for

20   ENVs).

21   We jointly estimated the Xs (X, X_1, X_2 and X_3), S and T in each population separately,

22   using candidate SNPs defined genome-wide (top 1% of SNPs) and empirical ORs corrected

23   for genomic variation in coverage, mutation and recombination rates, as recommended

24   (Kudaravalli, et al. 2009) (Supplementary Fig. S9, Online Methods). In every population

25   analyzed, the combination of these six empirical ORs used were found compatible with the

1 simulated ORs outputted by the ABC model (Supplementary Fig. S10). We found a very

2 limited numbers of selective sweeps (Fig. 3, Supplementary Fig. S11, see also the posterior

3 predictive checks shown in Supplementary Fig. S12). For example, we estimated 65 [CI:37-

4 96], 82 [CI:44-123] and 78 [CI:42-115] sweeps in the YRI, CEU and JPT (Japan) populations

5 (Fig. 3A-C). For comparison, 810, 1,013 and 1,059 selective sweeps were previously found in

6 these populations respectively (Schrider and Kern 2017). Overall, we estimated 62 [CI:36-

7 91], 71 [CI:35-111] and 88 [CI:50-127] sweeps on average for the African, European and

8 Asian continents (the estimates obtained in each population can be found in the

9 Supplementary Table S2).

10

11 **Robustness of the estimated numbers of selective sweeps**

12 We checked the robustness of the estimations of X obtained in our first round of estimations

13 shown in Fig. 3. First, we found consistent results using different combinations of summary

14 statistics (Supplementary Fig. S13). We next checked the effects of potential demographic

15 misspecifications (Supplementary Figs. S14-17). We adopted a strategy based on stress tests

16 to evaluate the differences in numbers of estimated sweeps obtained when drastically

17 modifying the demographic assumptions, e.g., replacing an expansion with a bottleneck or

18 largely increasing bottleneck intensities (we used models in the range of demography

19 previously inferred in human). We assessed this by swapping empirical and simulated ORs

20 from differing continental regions, e.g., analyzing the African 1000G populations using ORs

21 simulated under an Asian demographic model and inversely. Above all, we found very similar

22 numbers of sweeps when setting such incorrect demographic scenarios in the model

23 (Supplementary Figs. S15-16, details can be found in the Supplementary Table S2). The

24 higher values of X estimated in Africa under an Asian demographic model, i.e., 85 [CI:51-

25 121] (Supplementary Fig. S15) *vs* 62 [CI:36-91] sweeps on average, are simply due to lower

1   simulated ORs (see the simulated ORs under African and Asian demography in Fig. 1B). The

2   new estimations of X are increased because simulated ORs generated by larger X provide now

3   a better fit with empirical ORs (see the graphical explanations given in Supplementary Fig.

4   S14). We also re-analyzed the 1000G European populations under an Asian demographic

5   model (Supplementary Fig. S16), i.e., now setting a bottleneck four times stronger than in our

6   first round of estimations. The new estimations of X are only slightly increased, i.e., 83

7   [CI:48-120] (Supplementary Fig. S16) *vs* 71 [CI:35-111] sweeps on average, because ORs

8   simulated under an Asian demography are only slightly lower than under an European

9   demography (see also Fig. 1B and Supplementary Fig. S14). By symmetricity, we obtained

10   smaller estimated X in Asia when assuming a European demography (Supplementary Figs.

11   S14 and S16). Finally, we also modified several technical steps all at once, i.e., we set a 10%

12   higher recombination rate in ENVs than in PSVs (Kong, et al. 2010), excluded selection

13   signal found in ENVs (excluding ENVs in regions significantly enriched in candidate SNPs)

14   and used empirical 1000G ORs computed merging all chromosomes together. We also found

15   very similar, albeit slightly decreased, estimations of X (highly overlapping CIs when

16   comparing with the first round of estimations, Supplementary Fig. S18).

17   Our stress tests confirmed the very limited numbers of sweeps found in this study.

18   Notably, almost all re-estimated X fall within the 95% CIs boundaries of the initial

19   estimations. Because a true demographic model does not exist, we did not used other models

20   previously inferred in humans to re-estimate X (every inferred model poorly reproduces or

21   totally ignores a given component of the human demography). We acknowledge that new

22   estimations of X performed under other demographic models will differ but, given the low

23   differences in numbers of sweeps found in our stress tests, they should not change in large

24   proportions. What is of importance in the context of this study is that the very limited

25   numbers of sweeps found cannot be explained by poorly inferred demographic parameters

16

1 (see the little biases expected when assuming four time stronger/weaker bottlenecks than in

2 reality, Supplementary Fig. S17).

3

4 **Limited numbers of sweeps when also considering complete sweeps**

5 For reasons mentioned above, our first round of estimations was performed considering

6 incomplete sweeps only whereas the high numbers of soft sweeps previously detected mainly

7 refer to complete sweeps (Schrider and Kern 2017). We thus relaxed our assumption by

8 simulating both complete and incomplete selective sweeps using flat prior distributions for t,

9 as assumed previously (Schrider and Kern 2017), and several priors for s. The estimates

10 obtained under these priors, including the flat prior for s previously used (Schrider and Kern

11 2017), are given in the Supplementary Fig. 19 and Supplementary Table S2. When

12 considering priors enriched in small s values by using an equal mix between a Gamma

13 distribution (60% of $s \leq 0.01$) (Boyko, et al. 2008) and a L-shape distribution (90% of $s \leq 0.01$),

14 our method also provides unbiased estimations of X (Fig. 4A), since the ORs also reflect the X

15 (Fig. 4B). As expected, the new estimated values of X are increased with respect to our first

16 round of estimations, i.e., 115 [CI:68-160] and 165 [CI:119-211] sweeps on average in

17 Europe and Asia (Fig. 4C, Supplementary Table S2), because of lower simulated ORs (Fig.

18 4B), in agreement with the reduced power to detect sweeps at fixation using neutrality

19 statistics such as iHS (Voight, et al. 2006). However, our estimations are still far from the

20 thousand of sweeps previously estimated per non-African population (Schrider and Kern

21 2017).

22

23 **A trend toward more sweeps among non-African populations**

24 As expected given the higher derived allele frequencies (DAFs) observed outside Africa

25 (Coop, Pickrell, Novembre, et al. 2009) we found a non-significant trend toward younger

1   selection of higher intensity in non-Africans (overlapping CIs of the S and T estimates, Fig.

2   3E-F, Supplementary Table S2). For example, our S estimates (obtained assuming incomplete

3   sweeps only) were found higher in CEU than in YRI, i.e., 0.015 [CI:0.01-0.03] vs 0.09 [CI:0-

4   0.02], in agreement with previous estimations (0.034 vs 0.022 in the same populations

5   (Hawks, et al. 2007)). Our estimates are significantly lower likely because the selection

6   models assumed differ (dominant model vs additivity in the present study). Moreover, our

7   method may underestimate S when selection is strong as acknowledged above

8   (Supplementary Fig. S3). We also found a trend toward more sweeps among non-African

9   populations, particularly in Asia (Fig. 3A-C). For example, we estimated 68 [CI:46-91] and

10 165 [CI:119-211] sweeps in average in Africa and Asia respectively when including complete

11 sweeps in our model (Supplementary Table S2). As the non-African estimates of X_2 and X_3

12 were consistently found higher than in Africa (Fig. 3D and Supplementary Figs. S18-19), our

13 results also suggest more soft sweeps with low and intermediate initial frequencies

14 ($0.01 \leq p_{start} < 0.2$, $X_2 + X_3$) in Eurasian populations. Our estimations of higher numbers of

15 sweeps in Eurasians populations are in agreement with greater numbers of sweeps detected

16 outside Africa (Granka, et al. 2012; Pybus, et al. 2015; Schrider and Kern 2016).

17

18 **Selection signals in 1000G populations tend to be continent-specific**

19 The method used here relies on genome-wide enrichment of candidate SNPs of selection in

20 extended genic regions. We thus determined the genomic regions which contribute to this

21 genome-wide enrichment, i.e., those enriched in candidate SNPs for the same neutrality

22 statistics as used in our ABC estimations (Online Methods). We found that the most enriched

23 genomic regions contain multiple iconic examples of positive selection, e.g., the *LCT* region

24 in northern Europeans (Bersaglieri, et al. 2004), *EDAR* in all Asian populations and *TLR5* in

25 Africa (Grossman, et al. 2013), as well as various other examples including genes associated

1   with lighter skin pigmentation (Supplementary Text, see the most enriched genomic regions

2   in Supplementary Table S3). This indicates that the information underlying our estimations

3   corresponds to genomic signals in line with natural selection. We next investigated the

4   overlap of these enriched genomic regions across populations (Online Methods) to roughly

5   estimate the number of sweeps in humans as a whole. We found virtually no overlap between

6   populations from different continents (Supplementary Fig. S20), with some exceptions that

7   are indicated in Supplementary Fig. S21A and Supplementary Table S3. In contrast, the most

8   enriched regions tend to be shared across populations from the same continent

9   (Supplementary Fig. S20, Supplementary Table S3, an example given in Supplementary Fig.

10 S21B). These results indicate that the total number of sweeps in humans should be close to

11 the summation of the mean X computed per continent; i.e., 221 [CI:122-329] (Supplementary

12 Table S2), a first order approximation neglecting some selection signals shared across

13 continents and considering sweeps are highly shared within continents.

14

Discussion

16 Our study revealed very limited numbers of selective sweeps in humans regardless the

17 selection model considered (i.e., considering or not complete sweeps). We did not use

18 McDonald–Kreitman-based methods since such methods aim to infer adaptation rate since

19 divergence with other primate species (Uricchio, et al. 2019), and are potentially weakly

20 sensitive to recent selective sweeps within species (Messer and Petrov 2013). Instead, we

21 implemented an *ad hoc* ABC method to formally quantify numbers of selective sweeps over

22 shorter time spans (~100,000ya). This method does not scan genomic regions separately and

23 thus cannot provide lists of genomics region under selection (normal genome-wide scans can

24 be conducted in parallel, as we did in this study). It nevertheless helps to alleviate the load of

25 false positives described in introduction (weakly or moderately stringent detection thresholds

19

1   used to capture some sweeps of weak intensity provide large numbers of sweeps mainly

2   explained by false discoveries while highly stringent thresholds used to discard false positives

3   provide low numbers of detected sweeps poorly representative of the extent of selection

4   operating in populations). Here, using selection signals at 1% threshold we showed that

5   convenient statistics such as the OR for selection can provide suitable information to quantify

6   real numbers of selective sweeps in populations. Note that a similar ABC method can be

7   implemented using more than six ORs when background selection is explicitly simulated in

8   the ABC model, including ORs computed for F_{ST}, AFS-based statistics and others (the

9   expected gain in accuracy remains to be formally assessed).

10   Our estimations are not perfect and can still be improved. For example, we may have

11   missed some selective sweeps hidden in regions not yet classified as functional (selection

12   signals found in empirical ENVs downward bias the X estimations by decreasing the

13   empirical ORs). However, 70% of the genome was considered as potentially influenced by

14   selection and all significant signals of positive selection found in intergenic regions have been

15   accounted for (e.g., Supplementary Fig. S18), suggesting that we captured a large fraction of

16   the existing selective sweeps. Simulating whole chromosomes is still barely tractable in term

17   of computation times. We thus concatenated shorter simulated regions together, trimming

18   their edges and avoiding computation of any neutrality statistics across the junctions. This

19   insures that haplotype-based statistics were computed over linked SNPs simulated according

20   to human recombination rates. The demographic model assumed incorporates major

21   components of human demography (e.g., expansion, bottleneck and isolation-with-migration)

22   but some other aspects are ignored, such as the admixture with ancient hominids. However,

23   we found low differences in simulated ORs obtained with contrasting demographic histories,

24   we found similar estimations of X when replacing an expansion with a bottleneck, and only

25   slight overestimations of X when the bottleneck assumed is four times stronger than in reality.

20

1   Although we do not wish to claim that we have found the exact numbers of selective sweeps

2   (as if the demography was exactly known), our results indicate that the limited numbers of

3   sweeps estimated herein are not due to our demographic assumptions. Note that discrepancies

4   between point estimates across populations of the same continents must be interpreted with

5   cautious in term of selection (point estimates with highly overlapping CIs should be

6   considered as indistinguishable). They are likely explained by local demographic specificities

7   that are not properly accounted by the model (e.g., X was sometime found lower in FIN than

8   in CEU potentially because of a stronger bottleneck in the Finnish population (Bulik-Sullivan,

9   et al. 2015)).

10   A main result of our study is the very limited numbers of selective sweeps inferred over

11   the last ~100,000 years, even when modelling both complete and incomplete sweeps. It is

12   worth mentioning that our method can estimate X despite being based on neutrality statistics

13   that cannot even be computed when the selected alleles are fixed, e.g., iHS (even lower, ORs

14   are informative because the relationship with X is maintained). This illustrates the importance

15   of defining as PSVs the SNPs nearby selection targets because our method uses information at

16   linked sites through the enrichment of candidate SNPs around the fixed selected alleles.

17   Assuming similar sweep completion times (ranging from 0 to 3,000 generations) and similar

18   initial frequencies of selected alleles (ranging from $1/2N$ to 0.2), we estimated a much lower

19   number of selective sweeps in Europe and Asia (115 [CI:68-160] and 165 [CI:119-211]

20   respectively) than previously detected in CEU (~1,013 sweeps) and JPT (~1,059 sweeps)

21   (Schrider and Kern 2017). Beside our estimations, ~1,000 sweeps should result in simulated

22   ORs too large to be compatible with the empirical ORs observed (Fig. 1B, Fig. 4B),

23   suggesting that the majority of these predicted soft sweeps can be explained as mis-classified

24   neutral regions, as pointed by (Harris, et al. 2018). Nevertheless, even though we voluntary

25   considered the same time span as used by Schrider and Kern in their training simulated

21

datasets we may have missed some older selection signals that could be captured by their machine learning algorithm (our CIs should be enlarged when considering older selection ages in our ABC model). In addition, we also estimated, except in Africa, lower numbers of sweeps than previously detected based on another machine learning algorithm (355 and 424 detected sweeps in CEU and CHB respectively (Pybus, et al. 2015)). Apart from the sensitivity to false positives of this method based on detected/classified sites, such discrepancies are difficult to interpret because the machine learning algorithm has been trained using hard sweeps only, ignoring the soft sweep model.

More generally, we showed that our method can easily be extended to incorporate complete sweeps. In doing so, we estimated ~twice more selective sweeps in Eurasia than assuming complete sweeps only, e.g., 165 vs 88 sweeps in Asia (Supplementary Table S2). Our results thus suggest limited numbers of complete sweeps over the last ~100,000 years (e.g., at most 165 complete sweeps in Asia) and confirm that recent human adaptation has also been driven by a significant fraction of incomplete sweeps, some of them potentially ongoing (Wilde, et al. 2014; Field, et al. 2016). (Nearly all iconic sweeps are associated with a putative advantageous mutations still segregating in current generations (Vitti, et al. 2013; Jeong and Di Rienzo 2014; Fan, et al. 2016)). A similar ABC approach can be further designed to formally estimate the numbers of complete and incomplete sweeps specifically.

We also estimated a majority of sweeps with initial frequencies greater than 1% ($0.01 \leq p_{start} < 0.2$, $X_2 + X_3$), the rest being sweeps on very rare standing variants ($1/2N \leq p_{start} < 0.01$, X_1). Given the known difficulty to distinguish between hard and soft sweeps even for initial frequencies ranged to 0.2 (see some high miss-classification rates in (Schrider and Kern 2017; Harris, et al. 2018)), we did not provide separate estimates of the numbers of hard and soft sweeps on very rare standing variants. The numbers of hard sweeps remain unknown and may thus range from 0 to the estimated value of X_1. However, our

1 results ($X_1 < X_2 + X_3$) confirm soft sweeps as main drivers of human adaptation relative to hard

2 sweeps (Schrider and Kern 2017) (some examples have already been described in humans

3 (Peter, et al. 2012) and also in drosophila (Garud, et al. 2015), the latter have been discussed

4 in (Harris, et al. 2018)). Nevertheless, we only observed a moderate excess of sweeps on

5 standing variants with frequency higher than 1% ($X_2 + X_3 \approx 2/3 X$) because the proportion of

6 mutations with frequency greater than 1% drastically drops, as predicted by theory and

7 consistent with what is observed in extant populations (a mutation becomes advantageous

8 irrespective to its frequency). It is worth mentioning that we also found greater numbers of

9 such soft sweeps outside Africa (see the X_2 and X_3 estimated, Fig. 3D and Supplementary Fig.

10 S19A). It is not necessary to assume biological features or changes in selective regimes in

11 Eurasia since the proportion of such sweeps also depends on the demography of the

12 populations considered. Indeed, the loss (by genetic drift) of selected alleles at very low

13 frequency during the first generations of selection may be exacerbated in bottlenecked

14 populations relative to expanding populations. This may causes diminished numbers of

15 sweeps on very rare variants in Eurasian populations relative to Africa, and consequently, a

16 mechanical excess of sweeps on the other standing variants (with frequency higher than 1%)

17 outside Africa.

18   We would-like to emphasize that the scenario of positive selection on standing variation

19 investigated here is not related to polygenic adaptation (Pritchard and Di Rienzo 2010;

20 Pritchard, et al. 2010). Because biological processes likely differ (very few advantageous

21 alleles with large phenotypic effects *vs* many advantageous alleles with small phenotypic

22 effects), soft sweeps drive to fixation while polygenic adaptation refers to moderate changes

23 of selected allele frequencies only (Pritchard, et al. 2010). Hence, the neutrality statistics used

24 in this study, which are poorly sensitive to small changes in allele frequencies, do not capture

25 the pervasive effects of polygenic adaptation in humans (Field, et al. 2016). Instead, the

23

1   number of selective sweeps we report should be interpreted as the minimum number of

2   sweeps having occurred in a population. For example, given the important reproductive

3   function of the *SPAG4* gene (Kracklauer, et al. 2010), the species-wide selection signal found

4   near this gene (Supplementary Fig. S21A) is consistent with a single selection hit in each

5   continent independently. However, other functional variants found near the *SPAG4* region

6   suggest a more complex scenario in Asia, involving several independent selection hits in the

7   Asian lineage specifically, e.g., regulatory variants of *GDF5* have also been found under

8   selection in Asia (Capellini, et al. 2017).

9   Finally, the higher numbers of sweeps we estimated in non-African populations support

10   models in which more adaptation is expected when populations colonize new environments.

11   In an already colonized environment, populations also need to adapt to environmental

12   pressures that can change over time. The continent-specific signal of selection shared among

13   all European populations, encompasses eQTLs downregulating the expression of the *PLEK2*

14   gene (Supplementary Fig. S21B) in skin cells exposed to the sun (GTEx database, (Ardlie, et

15   al. 2015)). The cold paleoclimate (last ice age, from ~110 to ~10kya (Cooper, et al. 2015))

16   favored both light skin pigmentation and increased sensitivity to UV-induced melanoma in

17   Europe (Lopez, et al. 2014; Key, et al. 2016) while low expressions of *PLEK2* may increase

18   the survival probability in melanoma patients (Supplementary Text). The alleles

19   downregulating *PLEK2* could have been favored by selection during the late Pleistocene

20   climatic warming (~20 to ~10kya), as supported by selection signal of ~1-1.2Mb suggesting a

21   recent onset of selection that may coincide with the increase of regional temperatures and

22   solar luminosity in the northern hemisphere (Luo, et al. 2011) (Supplementary Text).

23   Our study provides independent lines of evidence that selective sweeps, despite their

24   small numbers with respect to other modes of adaption such as negative selection or

25   polygenic adaptation, enabled human populations to adapt to environmental pressures. The

1 method proposed can be applied in other species (e.g., Drosophila (Garud, et al. 2015), mouse

2 (Ihle, et al. 2006), domesticated animal breeds (Stella, et al. 2010; Roux, et al. 2015),

3 domestic dogs (Freedman, et al. 2016) and horses (Librado, et al. 2015)) and extended to

4 other modes of selection (e.g., adaptive introgression from ancient hominids or short-term

5 balancing selection), allowing for broader investigations of the impact of extreme

6 environments, domestication or mode of reproduction on recent adaptive evolution of species.

7

1   **Materials and Methods**

2   **1000 Genomes populations analyzed**

3   Analyses were performed on the 1000 Genomes Project phase 3 data, focusing on African,

4   European and Asian populations. We analyzed 1,511 individuals from five African, five

5   European and five East-Asian populations (85 to 113 individuals per population,

6   Supplementary Table S1), excluding populations with diverse continental or admixed

7   ancestry, for which little demographic history information was available. We downloaded

8   phased data obtained with SHAPEIT2 (Delaneau, et al. 2012), ancestral/derived states and

9   VEP annotations from the 1000G Project website.

10

11   **Simulating WGSs**

12   We carried out computer simulations of WGSs with various X values, ranging from 0

13   (neutrality) to >200 per population. The simulated WGSs mimicked the 1000G data, with

14   millions of SNPs spread over the genomes of ~100 unrelated individuals per population. As

15   we focused on the adaptive history of African, European and Asian populations in this study,

16   we systematically simulated triplets of populations according to inferred models of African,

17   European and Asian demography: the population with X loci under positive selection and two

18   other neutral populations (X=0), used as a reference for computations of interpopulation

19   neutrality statistics. Specifically, we used a three-populations isolation-with-migration model

20   (the parameters used can be found in (Grossman, et al. 2013)). This model incorporates an

21   ancient African expansion, an Out-of-Africa exodus ~100 kya (28 years per generation

22   (Fenner 2005; Moorjani, et al. 2016)) followed by a bottleneck and a split of Eurasians into

23   European and Asian populations ~58kya. This model also reproduces different migration rates

24   between continents, with a probability of the order of 10^{-5} per haploid genome per generation.

26

1   One key feature is the presence of two population bottlenecks in non-African populations, the

2   second bottleneck being stronger in the Asian population (Pickrell, et al. 2009b).

3   We used SLiM (Haller and Messer 2017) to simulate 5Mb regions sequenced in 100

4   unrelated individuals per population, using human recombination rates sampled from the

5   HapMap recombination maps (Frazer, et al. 2007). We simulated 10^4 neutrally evolving DNA

6   regions and 2×10^3 selected DNA regions. For each triplet of populations, we simulated

7   selection in the population of interest (African, Asian or European) by inserting (in the middle

8   of the region) an advantageous mutation at generation t, with a frequency, p_{start}, ranging from

9    $1/2N$ to 0.2 as previously assumed (Schrider and Kern 2017). The p_{start} was randomly drawn

10   from the allele frequency spectrum at the generation t. The intensities and ages of selection

11   were randomly drawn from specified distributions (see main text). It is worth mentioning that

12   we simulated long DNA regions to avoid premature truncation because selection signals can

13   extent over mega bases for selection events, particularly recent and/or strong events, i.e.,

14   ~2Mb in the LCT region (various estimates of s for rs4988135 ranged from 0.025 to 0.069

15   (Tishkoff, et al. 2007; Peter, et al. 2012; Chen, et al. 2015)). Because SLiM is a forward-in-

16   time simulator, the computation times, which depend on both the effective population size N

17   and the t generations simulated, are large for the model investigated. We therefore optimized

18   computational times by rescaling effective population sizes and times according to N/λ and

19   t/λ with $\lambda = 10$ (Hoggart, et al. 2007). We used rescaled mutation and recombination rates,

20    $\lambda\mu$ and λr. Similarly, because we divided the number of generations by λ, the selection

21   parameter s must be multiplied by the same factor (Hoggart, et al. 2007; Haller and Messer

22   2017). Finally, WGSs were obtained by concatenating randomly drawn 5Mb regions, some of

23   which were considered to be ENVs, the rest being PSVs (see below). We built WGSs by

24   restricting the X simulated sweeps to PSV regions, because ENV genomic regions are, by

27

1   definition, neutral. The ABC simulations used for estimations are simulated sets of such

2   WGSs (10^5 simulated WGSs, the prior distributions used for *X*, *S* and *T* are specified below).

3

4   **PSVs in simulated WGSs**

5   PSVs (Supplementary Fig. S1A) are all sites potentially influenced by selection either directly

6   (all potential targets of selection, i.e. all variants altering phenotypes in real data) or indirectly

7   (all neutral SNPs in the vicinity of a potential target of selection). The probability ξ_i that the

8   i^{th} SNP is influenced by selection starts from 0 (neutral SNP far from the potential targets of

9   selection) and increase to 1 when approaching a potential target of selection. In this analysis,

10   we discretized this probability by considering an indicator variable I_i, assigned to SNP *i* and

11   equal to 1 (PSV) or 0 (ENV):

12
$$I_i \begin{cases} 1 \text{ when } \xi_i > 0 & ;\ PSV \\ 0 \text{ when } \xi_i = 0 & ;\ ENV \end{cases}$$

13   In simulated WGSs, the PSVs are randomly simulated as tracts of SNPs with I_i=1 randomly

14   spread over the genomes. We reproduced the same proportion of PSVs as observed in 1000G

15   populations, with numbers of simulated SNPs per population matching those observed in

16   1000G populations. In our simulations the recombination rates are randomly sampled in

17   human recombination maps and are thus similar across PSVs and ENVs. However, in real

18   data the recombination rate is lower in genes than in intergenic regions. Initially lower in

19   genes it suddenly increases in flanking regions and progressively decreases with distance

20   from the nearest gene to become lower in remote intergenic regions (Myers, et al. 2005;

21   Coop, et al. 2008; Kong, et al. 2010), making our simulations conservative with respect to the

22   rates of candidate SNPs in ENVs far from genes. We however also tested higher

23   recombination rates in ENVs than in PSVs (Kong, et al. 2010) and re-estimated the

24   parameters accordingly (supplementary Fig. S18).

1

Neutrality statistics and candidate SNPs in simulated WGSs

For each simulated WGS, we computed several widely used neutrality statistics expected to

have extreme values for SNPs targeted by selection or located close to such SNPs. We used

haplotype-based neutrality statistics, which compare the haplotypes carrying the derived and

ancestral alleles, iHS, DIND, ΔiHH, and the derived alleles between populations, XP-EHH.

We also used the Fay and Wu's *H*, which detect deviations from the neutral allele frequency

spectrum (AFS) in short genomic regions. We used a sliding-windows approach (100 kb

windows centered on each SNP (Fagny, et al. 2014)) for these computations. The sliding-

windows began and ended 50kb from the edges of the 5Mb simulated regions, to prevent

truncation in the 100 kb sliding windows (a similar approach was applied to the 1000G

chromosomes). As iHS, DIND, ΔiHH and XP-EHH are sensitive to the inferred

ancestral/derived state, we computed these statistics only when the derived state was

determined unambiguously (Fagny, et al. 2014) (i.e. more than 95% of SNPs). We then

normalized these statistics by DAF bin (Voight, et al. 2006; Fagny, et al. 2014) (mutations

grouped by DAF bin, from 0 to 1, in increments of 0.025). We minimized the false-positive

discovery by excluding SNPs with a DAF below 0.2, as the power to detect positive selection

has been shown to be limited at such low frequencies (Voight, et al. 2006; Fagny, et al. 2014).

The method used are implemented in selink, a software to detect selection using whole-

genome datasets (https://github.com/h-e-g/selink). Finally, for each neutrality statistic, we

defined candidate SNPs of selection as the 1% of SNPs with the most extreme values over 10^4

neutral simulations. For iHS, DIND, ΔiHH and XP-EHHs, we considered extreme values

indicative for selection targeting the derived alleles, e.g, large negative values of iHS indicate

unusually long haplotypes carrying the derived allele.

29

1   We choose these neutrality statistics because the widespread effects of background

2   selection may be confounded with positive selection as mentioned in the main text. For

3   example, the Tajima's D is sensitive to BGS (Zeng, et al. 2006) and the differences in allele

4   frequencies between-population are expected to be exacerbated in regions affected by BGS, a

5   pattern that can be confounded with positive selection (Coop, Pickrell, Novembre, et al. 2009;

6   Pickrell, et al. 2009b; Pritchard, et al. 2010). We excluded F_{ST}, Tajima's D and others

7   similarly affected by BGS. We only retained Fay and Wu's H and the haplotype-based

8   statistics previously found to be insensitive to BGS (Zeng, et al. 2006; Fagny, et al. 2014),

9   e.g., haplotype-based statistics compare haplotypes carrying the derived allele with those

10   carrying the ancestral alleles as internal controls that should be affected by BGS to a similar

11   extent. We used this approach (excluding statistics sensitive to BGS) rather than simulating

12   widespread BGS, because we aimed to avoid bias in our ABC estimations due to the

13   imperfectly known patterns of BGS on the human genome.

14

15   **Odds ratio for selection used as ABC summary statistics**

16   The summary statistics used in the present study were the odds ratio for selection

17   (Kudaravalli, et al. 2009; Fagny, et al. 2014), computed for the population of interest (with X

18   simulated or estimated), for each WGS (simulated or 1000G) and each neutrality statistic

19   separately. Each OR assesses the enrichment of candidate SNPs in PSVs, as follows:

20
$$OR = \left[\frac{P(PSV|Candidate)}{P(PSV|\overline{Candidate})} \right] \left[\frac{P(ENV|\overline{Candidate})}{P(ENV|Candidate)} \right],$$

21   with $Candidate$ and $\overline{Candidate}$ being candidate and non-candidate SNPs, respectively (see

22   above). The OR is greater than 1 if positive selection has preferentially occurred in functional

23   regions, because such selection tends to increase the number of candidate SNPs across the

24   selective sweep regions (Voight, et al. 2006).

30

1

ABC prior distributions, acceptance rules and accuracy validation

We randomly draw X from a uniform prior distribution $X \sim U(0, > 200)$, where X=0 is a neutral WGS. Priors for mean intensity and age, S and T, were derived from the priors for s and t used to simulate the X sweeps (the priors used are indicated in main text). We used the 'abc' R package and the standard ABC method (Beaumont, et al. 2002), in which posteriors are constructed from simulated parameters accepted and adjusted by local linear regression (method="Loclinear" in the 'abc' package). The accepted simulated parameters are those which provide the best fit with empirical data (the 'abc' parameter 'tol' was set to be equal to 0.005). We used the mean of the posterior distribution as point estimate and provided the 95% credible interval boundaries (computed from the posterior distribution).

To test the accuracy of our estimations, we compared the estimated and simulated parameter values, $\hat{\theta}_i$ and θ_i respectively, using classical accuracy indices: the relative error rE (i.e. difference between estimated and true values, expressed as a proportion of the true value, $rE = (\hat{\theta}_i - \theta_i)/\theta_i, i = 1, \dots, J$), the relative root of the mean square error, $rRMSE$ (i.e. the root of the MSE expressed as a proportion of the true value), and the proportion of true values within the 90% credible interval of estimates, $90\%COV = \frac{1}{J}\sum_1^J 1(q_1 < \theta_i < q_2)$ where $1(C)$ is the indicative function (equal to 1 when C is true, 0 otherwise) and q_1 and $q_{2,}$ the corresponding percentiles of the posterior distributions.

Defining PSVs in the 1000G data

The definition of the PSVs in the 1000G populations is based on the VEP (Ensembl Variant Effect Predictor, Supplementary Fig. S8) annotations provided by the 1000G website. We included in PSVs the potential targets of selection as exhaustively as possible. We considered as PSVs missense variants, stop-gained mutations and all the regulatory variants, including

31

1   SNPs located in the regions 5' and 3' to genes (regions expected to be enriched in eQTLs)

2   together with the transcription factor binding sites located farther away from genes. As in

3   simulations, we included all SNPs located in the vicinity of these potential direct targets of

4   selection to take into account the hitchhiking effects of selection at nearby linked loci. For

5   example, in the case of the high-altitude adaptation in humans, two of the largest Tibetan-Han

6   frequency differences found in EPAS1 were annotated as intronic (Yi, et al. 2010). Hence, all

7   synonymous, intronic, 5' and 3'UTR SNPs (i.e., ~50% of annotated SNPs) are included in

8   PSVs. We also included upstream/downstream SNPs in PSVs to prevent early truncations of

9   selective sweep signals. With such filters, ~70% of 1000G SNPs were considered to be PSVs.

10   Finally, some particular cases are hardly tractable based on VEP annotation only. These

11   include the selected sites that are unknown functional variants annotated as intergenic, small

12   regulatory regions located far from other PSVs and regulatory variants located in edges of

13   PSVs tracts. In these situations, selection signals may be found in ENV and therefore can bias

14   downward our estimations (selection signals found in ENV cause lower empirical ORs). To

15   minimize such estimation biases, we annotated as PSVs all the SNPs with a genome-wide

16   significant enrichment in candidate SNPs (this enrichment is computed using 100 kb centered

17   on every SNP, see below). High enrichment are indicative of selection, since, as stated above,

18   positive selection produces clusters of candidate SNPs (Voight, et al. 2006). This step has

19   only a marginal effect on the total number of SNPs classified as PSVs (~0.01% of SNPs

20   reallocated), but it can inflate neutral ORs (e.g., OR computed for iHS from purely neutral

21   simulations, $X=0$, is equal to 1.2 rather than 1). We therefore reproduced this step in the

22   simulations used to obtain ABC estimations for 1000G populations, i.e., the simulated SNPs

23   annotated as PSVs included all simulated SNPs with a significant enrichment in candidate

24   SNPs. We also performed a round of estimation after removing from the analysis all ENVs

25   with a significant enrichment in candidate SNPs of selection (supplementary Fig. S18).

32

1

Odds ratio for selection in the 1000G populations

When analyzing the 1000G populations, we computed the ORs using a logistic regression to

control for several covariates (Kudaravalli, et al. 2009), including genomic variation in

sequencing quality, recombination and mutation rates. For each neutrality statistic and

chromosome, we set

$$Logit[I(PSV = 1)]$$

$$= \beta_1 I(Candidate\ SNP = 1)$$

$$+ [\ \beta_2 Cov + \beta_3 Rec + \beta_4 NbSNP\ + \beta_5 Cov * Rec\ +\ \beta_6 Rec * NbSNP$$

$$+\ \beta_7 NbSNP * Cov\ ] + \varepsilon$$

with I(PSV = 1), the indicator function, equal to 1 if the SNP is a PSV, or 0 otherwise,

I($Candidate\ SNP$ = 1) being an indicator function equal to 1 if the SNP is a candidate SNP

of selection or 0 otherwise (candidate SNPs are the 1% of SNPs with the most extreme values

genome-wide). Rec is the mean recombination rate in cM/bp (obtained from HapMap

recombination maps), Cov is the mean coverage, and NbSNP is the number of SNPs

computed with 100 kb sliding windows. The OR was estimated with exp(β_1) and averaged

over chromosomes (Kudaravalli, et al. 2009). We also performed a round of estimation using

empirical ORs computed merging all chromosomes together (supplementary Fig. S18).

Assessing the genomic regions enriched in candidate SNPs of selection

For each SNP and each of the six neutrality statistics used in the ABC estimations (see main

text), we computed the proportion of candidate SNPs in a 100 kb window around the SNP

being considered. We next determined the empirical *P*-values (*P*) for these proportions and

combined them into a single combined selection score (denoted by CSS) using a Fisher score,

1 $CSS = -2 \sum_1^6 \log(P_i)$ (Deschamps, et al. 2016). The rationale behind such a composite

2 approach (Grossman, et al. 2010; Grossman, et al. 2013; Deschamps, et al. 2016) is that

3 neutrality statistics are more strongly correlated for positively selected variants than for

4 neutral sites (Grossman, et al. 2013). Consequently, false positives may harbor extreme values

5 for a few neutrality statistics only, whereas SNPs genuinely selected (or nearby SNPs) should

6 harbor extreme values for several statistics together, a feature captured by the combined score.

7 Finally, the genomic regions enriched in candidate SNPs were defined as consecutive SNPs

8 with genome-wide significant CSS values (P<0.01). In these enriched regions, the strength of

9 selection signal has been related to the magnitude of the enrichment in candidate SNPs

10 through the maximum CSS value found in the region. Indeed, high combined selection score

11 values are expected for SNPs targeted by young and strong selection and for the others SNPs

12 nearby, e.g., SNPs nearby rs4988235 (*LCT* region) were found among the highest CSS values

13 found genome-wide (Supplementary Table S3).

14

15 **Assessing the overlap of selection signals between the 1000G populations**

16 For each region enriched in candidate SNPs of selection, we assessed the sharing of selection

17 signals between populations by mean of an overlap score, calculated as the number of

18 populations for which the same enriched region was identified. For each enriched region,

19 overlap scores were calculated both within and between continents (upper limits of 5 for

20 within-content and 10 for between-continent scores, because there were five populations from

21 each of three continents). Thus, continent-specific enriched regions would have within- and

22 between-continent overlap scores of 5 and 0 respectively, whereas population-specific

23 enriched regions would have within- and between-continent overlap scores of 1 and 0,

24 respectively.

25

34

1 **URLs**

2 1000 Genomes data: ftp://ftp.1000genomes.ebi.ac.uk/vol1/ftp/release/20130502/, ancestral

3 state,

4 ftp://ftp.ncbi.nih.gov/1000genomes/ftp/technical/working/20120316_phase1_integrated_relea

5 se_version2/, VEP functional annotation,

6 ftp://ftp.ncbi.nih.gov/1000genomes/ftp/technical/working/20120316_phase1_integrated_relea

7 se_version2/.

8 tools for Approximate Bayesian Computation (ABC), http://cran.r-

9 project.org/web/packages/abc/index.html, GTEx (Genotype-Tissue Expression Project)

10 http://gtexportal.org/home/, DAA (Digital Aging Atlas) http://ageing-map.org/, the human

11 protein atlas http://www.proteinatlas.org, the American Cancer Society

12 https://www.cancer.org/, NCBI gene database https://www.ncbi.nlm.nih.gov/gene/26499

13

14 **Supplemental Data**

15 Supplemental data, including Figs. S1 to S21 and Tables S1 to S3 (Tables S2 and S3 are

16 supplied as Excel files) can be found with this article online.

17

4   **Author contributions**

9   **Competing financial interests**

12   **Corresponding authors**

13   Correspondence to: Guillaume Laval at glaval@pasteur.fr

14

1 **References**

2

3 Akey JM. 2009. Constructing genomic maps of positive selection in humans: where do we go

4   from here? Genome Research 19:711-722.

5 Ardlie KG, DeLuca DS, Segre AV, Sullivan TJ, Young TR, Gelfand ET, Trowbridge CA,

6   Maller JB, Tukiainen T, Lek M, et al. 2015. The Genotype-Tissue Expression (GTEx)

7   pilot analysis: Multitissue gene regulation in humans. Science 348:648-660.

8 Auton A, Brooks LD, Durbin RM, Garrison EP, Kang HM, Korbel JO, Marchini JL,

9   McCarthy S, McVean GA, Abecasis GR. 2015. A global reference for human genetic

10   variation. Nature 526:68-74.

11 Barreiro LB, Ben-Ali M, Quach H, Laval G, Patin E, Pickrell JK, Bouchier C, Tichit M,

12   Neyrolles O, Gicquel B, et al. 2009. Evolutionary dynamics of human Toll-like

13   receptors and their different contributions to host defense. Plos Genetics 5:e1000562.

14 Barreiro LB, Laval G, Quach H, Patin E, Quintana-Murci L. 2008. Natural selection has

15   driven population differentiation in modern humans. Nat Genet 40:340-345.

16 Beaumont MA, Zhang WY, Balding DJ. 2002. Approximate Bayesian computation in

17   population genetics. Genetics 162:2025-2035.

18 Bersaglieri T, Sabeti PC, Patterson N, Vanderploeg T, Schaffner SF, Drake JA, Rhodes M,

19   Reich DE, Hirschhorn JN. 2004. Genetic signatures of strong recent positive selection at

20   the lactase gene. American Journal of Human Genetics 74:1111-1120.

21 Boyko AR, Williamson SH, Indap AR, Degenhardt JD, Hernandez RD, Lohmueller KE,

22   Adams MD, Schmidt S, Sninsky JJ, Sunyaev SR, et al. 2008. Assessing the

23   evolutionary impact of amino acid mutations in the human genome. Plos Genetics

24   4:e1000083.

1   Bulik-Sullivan BK, Loh PR, Finucane HK, Ripke S, Yang J, Patterson N, Daly MJ, Price AL,

2   Neale BM. 2015. LD Score regression distinguishes confounding from polygenicity in

3   genome-wide association studies. Nat Genet 47:291-295.

4   Capellini TD, Chen H, Cao JX, Doxey AC, Kiapour AM, Schoor M, Kingsley DM. 2017.

5   Ancient selection for derived alleles at a GDF5 enhancer influencing human growth and

6   osteoarthritis risk. Nature Genetics 49:1202-+.

7   Chen H, Hey J, Slatkin M. 2015. A hidden Markov model for investigating recent positive

8   selection through haplotype structure. Theoretical Population Biology 99:18-30.

9   Coop G, Pickrell JK, Kudaravalli S, Novembre J, Myers RM, Cavalli-Sforza LL, Feldman

10   MW, Pritchard JK. 2009. Selection, drift, and geography in recent human evolution.

11   American Journal of Physical Anthropology:109-109.

12   Coop G, Pickrell JK, Novembre J, Kudaravalli S, Li J, Absher D, Myers RM, Cavalli-Sforza

13   LL, Feldman MW, Pritchard JK. 2009. The Role of Geography in Human Adaptation.

14   Plos Genetics 5.

15   Coop G, Wen XQ, Ober C, Pritchard JK, Przeworski M. 2008. High-resolution mapping of

16   crossovers reveals extensive variation in fine-scale recombination patterns among

17   humans. Science 319:1395-1398.

18   Cooper A, Turney C, Hughen KA, Brook BW, McDonald HG, Bradshaw CJ. 2015.

19   PALEOECOLOGY. Abrupt warming events drove Late Pleistocene Holarctic

20   megafaunal turnover. Science 349:602-606.

21   Delaneau O, Marchini J, Zagury JF. 2012. A linear complexity phasing method for thousands

22   of genomes. Nat Methods 9:179-181.

23   Deschamps M, Laval G, Fagny M, Itan Y, Abel L, Casanova JL, Patin E, Quintana-Murci L.

24   2016. Genomic Signatures of Selective Pressures and Introgression from Archaic

Hominins at Human Innate Immunity Genes. American Journal of Human Genetics 98:5-21.

Fagny M, Patin E, Enard D, Barreiro LB, Quintana-Murci L, Laval G. 2014. Exploring the occurrence of classic selective sweeps in humans using whole-genome sequencing data sets. Molecular Biology and Evolution 31:1850-1868.

Fan S, Hansen ME, Lo Y, Tishkoff SA. 2016. Going global by adapting local: A review of recent human adaptation. Science 354:54-59.

Fay JC, Wu CI. 2000. Hitchhiking under positive Darwinian selection. Genetics 155:1405-1413.

Fenner JN. 2005. Cross-cultural estimation of the human generation interval for use in genetics-based population divergence studies. American Journal of Physical Anthropology 128:415-423.

Ferrer-Admetlla A, Liang M, Korneliussen T, Nielsen R. 2014. On Detecting Incomplete Soft or Hard Selective Sweeps Using Haplotype Structure. Molecular Biology and Evolution 31:1275-1291.

Field Y, Boyle EA, Telis N, Gao ZY, Gaulton KJ, Golan D, Yengo L, Rocheleau G, Froguel P, McCarthy MI, et al. 2016. Detection of human adaptation during the past 2000 years. Science 354:760-764.

Frazer KA, Ballinger DG, Cox DR, Hinds DA, Stuve LL, Gibbs RA, Belmont JW, Boudreau A, Hardenbol P, Leal SM, et al. 2007. A second generation human haplotype map of over 3.1 million SNPs. Nature 449:851-861.

Freedman AH, Schweizer RM, Ortega-Del Vecchyo D, Han E, Davis BW, Gronau I, Silva PM, Galaverni M, Fan Z, Marx P, et al. 2016. Demographically-Based Evaluation of Genomic Regions under Selection in Domestic Dogs. Plos Genetics 12:e1005851.

1   Garud NR, Messer PW, Buzbas EO, Petrov DA. 2015. Recent Selective Sweeps in North

2   American Drosophila melanogaster Show Signatures of Soft Sweeps. Plos Genetics 11.

3   Granka JM, Henn BM, Gignoux CR, Kidd JM, Bustamante CD, Feldman MW. 2012. Limited

4   evidence for classic selective sweeps in African populations. Genetics 192:1049-1064.

5   Grossman SR, Andersen KG, Shlyakhter I, Tabrizi S, Winnicki S, Yen A, Park DJ, Griesemer

6   D, Karlsson EK, Wong SH, et al. 2013. Identifying recent adaptations in large-scale

7   genomic data. Cell 152:703-713.

8   Grossman SR, Shlyakhter I, Karlsson EK, Byrne EH, Morales S, Frieden G, Hostetter E,

9   Angelino E, Garber M, Zuk O, et al. 2010. A composite of multiple signals

10   distinguishes causal variants in regions of positive selection. Science 327:883-886.

11   Gunther T, Schmid KJ. 2011. Improved haplotype-based detection of ongoing selective

12   sweeps towards an application in Arabidopsis thaliana. BMC Res Notes 4:232.

13   Haller BC, Messer PW. 2017. SLiM 2: Flexible, Interactive Forward Genetic Simulations.

14   Molecular Biology and Evolution 34:230-240.

15   Harris RB, Sackman A, Jensen JD. 2018. On the unfounded enthusiasm for soft selective

16   sweeps II: Examining recent evidence from humans, flies, and viruses. Plos Genetics

17   14.

18   Hawks J, Wang ET, Cochran GM, Harpending HC, Moyzis RK. 2007. Recent acceleration of

19   human adaptive evolution. Proceedings of the National Academy of Sciences of the

20   United States of America 104:20753-20758.

21   Hermisson J, Pennings PS. 2005. Soft sweeps: Molecular population genetics of adaptation

22   from standing genetic variation. Genetics 169:2335-2352.

23   Hernandez RD, Kelley JL, Elyashiv E, Melton SC, Auton A, McVean G, Sella G, Przeworski

24   M. 2011. Classic selective sweeps were rare in recent human evolution. Science

25   331:920-924.

Hoggart CJ, Chadeau-Hyam M, Clark TG, Lampariello R, Whittaker JC, De Iorio M, Balding DJ. 2007. Sequence-level population simulations over large genomic regions. Genetics 177:1725-1731.

Hsieh P, Veeramah KR, Lachance J, Tishkoff SA, Wall JD, Hammer MF, Gutenkunst RN. 2016. Whole-genome sequence analyses of Western Central African Pygmy hunter-gatherers reveal a complex demographic history and identify candidate genes under positive natural selection. Genome Research 26:279-290.

Huff CD, Harpending HC, Rogers AR. 2010. Detecting positive selection from genome scans of linkage disequilibrium. BMC Genomics 11:8.

Ihle S, Ravaoarimanana I, Thomas M, Tautz D. 2006. An analysis of signatures of selective sweeps in natural populations of the house mouse. Molecular Biology and Evolution 23:790-797.

Innan H, Kim Y. 2004. Pattern of polymorphism after strong artificial selection in a domestication event. Proceedings of the National Academy of Sciences of the United States of America 101:10667-10672.

Jensen JD. 2014. On the unfounded enthusiasm for soft selective sweeps. Nat Commun 5:5281.

Jeong C, Di Rienzo A. 2014. Adaptations to local environments in modern human populations. Curr Opin Genet Dev 29:1-8.

Jin W, Xu S, Wang H, Yu Y, Shen Y, Wu B, Jin L. 2012. Genome-wide detection of natural selection in African Americans pre- and post-admixture. Genome Research 22:519-527.

Key FM, Fu Q, Romagne F, Lachmann M, Andres AM. 2016. Human adaptation and population differentiation in the light of ancient genomes. Nat Commun 7:10775.

Kimura M. 1977. Preponderance of synonymous changes as evidence for the neutral theory of molecular evolution. Nature 267:275-276.

Kong A, Thorleifsson G, Gudbjartsson DF, Masson G, Sigurdsson A, Jonasdottir A, Walters GB, Jonasdottir A, Gylfason A, Kristinsson KT, et al. 2010. Fine-scale recombination rate differences between sexes, populations and individuals. Nature 467:1099-1103.

Kracklauer MP, Wiora HM, Deery WJ, Chen X, Bolival B, Romanowicz D, Simonette RA, Fuller MT, Fischer JA, Beckingham KM. 2010. The Drosophila SUN protein Spag4 cooperates with the coiled-coil protein Yuri Gagarin to maintain association of the basal body and spermatid nucleus. Journal of Cell Science 123:2763-2772.

Kudaravalli S, Veyrieras JB, Stranger BE, Dermitzakis ET, Pritchard JK. 2009. Gene Expression Levels Are a Target of Recent Natural Selection in the Human Genome. Molecular Biology and Evolution 26:649-658.

Li HP, Stephan W. 2006. Inferring the demographic history and rate of adaptive substitution in Drosophila. Plos Genetics 2:1580-1589.

Librado P, Sarkissian CD, Ermini L, Schubert M, Jonsson H, Albrechtsen A, Fumagalli M, Yang MA, Gambo C, Seguin-Orlando A, et al. 2015. Tracking the origins of Yakutian horses and the genetic basis for their fast adaptation to subarctic environments. Proceedings of the National Academy of Sciences of the United States of America 112:E6889-E6897.

Lopez S, Garcia O, Yurrebaso I, Flores C, Acosta-Herrera M, Chen H, Gardeazabal J, Careaga JM, Boyano MD, Sanchez A, et al. 2014. The Interplay between Natural Selection and Susceptibility to Melanoma on Allele 374F of SLC45A2 Gene in a South European Population. Plos One 9.

Luo Y, Robinson S, Fujita J, Siconolfi L, Magidson J, Edwards CK, Wassmann K, Storm K, Norris DA, Bankaitis-Davis D, et al. 2011. Transcriptome profiling of whole blood cells identifies PLEK2 and C1QB in human melanoma. Plos One 6:e20971.

Maynard Smith J, Haigh J. 1974. The hitch-hiking effect of a favourable gene. Genetics Research 23:23-35.

Mcdonald JH, Kreitman M. 1991. Adaptive Protein Evolution at the Adh Locus in Drosophila. Nature 351:652-654.

Messer PW, Petrov DA. 2013. Frequent adaptation and the McDonald-Kreitman test. Proceedings of the National Academy of Sciences of the United States of America 110:8615-8620.

Moorjani P, Sankararaman S, Fu QM, Przeworski M, Patterson N, Reich D. 2016. A genetic method for dating ancient genomes provides a direct estimate of human generation interval in the last 45,000 years. Proceedings of the National Academy of Sciences of the United States of America 113:5652-5657.

Myers S, Bottolo L, Freeman C, McVean G, Donnelly P. 2005. A fine-scale map of recombination rates and hotspots across the human genome. Science 310:321-324.

Nakagome S, Alkorta-Aranburu G, Amato R, Howie B, Peter BM, Hudson RR, Di Rienzo A. 2016. Estimating the Ages of Selection Signals from Different Epochs in Human History. Molecular Biology and Evolution 33:657-669.

Orr HA, Betancourt AJ. 2001. Haldane's sieve and adaptation from the standing genetic variation. Genetics 157:875-884.

Pavlidis P, Alachiotis N. 2017. A survey of methods and tools to detect recent and strong positive selection. Journal of Biological Research-Thessaloniki 24.

Pennings PS, Hermisson J. 2006a. Soft sweeps II-molecular population genetics of adaptation from recurrent mutation or migration. Molecular Biology and Evolution 23:1076-1084.

Pennings PS, Hermisson J. 2006b. Soft sweeps III: The signature of positive selection from recurrent mutation. Plos Genetics 2:1998-2012.

Peter BM, Huerta-Sanchez E, Nielsen R. 2012. Distinguishing between Selective Sweeps from Standing Variation and from a De Novo Mutation. Plos Genetics 8.

Pickrell JK, Coop G, Novembre J, Kudaravalli S, Li JZ, Absher D, Srinivasan BS, Barsh GS, Myers RM, Feldman MW, et al. 2009a. Signals of recent positive selection in a worldwide sample of human populations. Genome Research 19:826-837.

Pickrell JK, Coop G, Novembre J, Kudaravalli S, Li JZ, Absher D, Srinivasan BS, Barsh GS, Myers RM, Feldman MW, et al. 2009b. Signals of recent positive selection in a worldwide sample of human populations. Genome Research 19:826-837.

Pritchard JK, Di Rienzo A. 2010. Adaptation - not by sweeps alone. Nature Reviews Genetics 11:665-667.

Pritchard JK, Pickrell JK, Coop G. 2010. The genetics of human adaptation: hard sweeps, soft sweeps, and polygenic adaptation. Curr Biol 20:R208-215.

Przeworski M, Coop G, Wall JD. 2005. The signature of positive selection on standing genetic variation. Evolution 59:2312-2323.

Pybus M, Luisi P, Dall'Olio GM, Uzkudun M, Laayouni H, Bertranpetit J, Engelken J. 2015. Hierarchical boosting: a machine-learning framework to detect and classify hard selective sweeps in human populations. Bioinformatics.

Roux PF, Boitard S, Blum Y, Parks B, Montagner A, Mouisel E, Djari A, Esquerre D, Desert C, Boutin M, et al. 2015. Combined QTL and Selective Sweep Mappings with Coding SNP Annotation and cis-eQTL Analysis Revealed PARK2 and JAG2 as New Candidate Genes for Adiposity Regulation. G3-Genes Genomes Genetics 5:517-529.

Sabeti PC, Varilly P, Fry B, Lohmueller J, Hostetter E, Cotsapas C, Xie X, Byrne EH, McCarroll SA, Gaudet R, et al. 2007. Genome-wide detection and characterization of positive selection in human populations. Nature 449:913-918.

1   Schaffner SF, Foo C, Gabriel S, Reich D, Daly MJ, Altshuler D. 2005. Calibrating a

2   coalescent simulation of human genome sequence variation. Genome Research

3   15:1576-1583.

4   Schmidt JM, de Manuel M, Marques-Bonet T, Castellano S, Andres AM. 2019. The impact of

5   genetic adaptation on chimpanzee subspecies differentiation. Plos Genetics

6   15:e1008485.

7   Schrider DR, Kern AD. 2016. S/HIC: Robust Identification of Soft and Hard Sweeps Using

8   Machine Learning. Plos One 11.

9   Schrider DR, Kern AD. 2017. Soft sweeps are the dominant mode of adaptation in the human

10   genome. Molecular Biology and Evolution.

11   Smith J, Coop G, Stephens M, Novembre J. 2018. Estimating Time to the Common Ancestor

12   for a Beneficial Allele. Molecular Biology and Evolution 35:1003-1017.

13   Stella A, Ajmone-Marsan P, Lazzari B, Boettcher P. 2010. Identification of selection

14   signatures in cattle breeds selected for dairy production. Genetics 185:1451-1461.

15   Tang K, Thornton KR, Stoneking M. 2007. A new approach for using genome scans to detect

16   recent positive selection in the human genome. PLoS Biol 5:e171.

17   Teshima KM, Coop G, Przeworski M. 2006. How reliable are empirical genomic scans for

18   selective sweeps? Genome Research 16:702-712.

19   Tishkoff SA, Reed FA, Ranciaro A, Voight BF, Babbitt CC, Silverman JS, Powell K,

20   Mortensen HM, Hirbo JB, Osman M, et al. 2007. Convergent adaptation of human

21   lactase persistence in Africa and Europe. Nat Genet 39:31-40.

22   Uricchio LH, Petrov DA, Enard D. 2019. Exploiting selection at linked sites to infer the rate

23   and strength of adaptation. Nat Ecol Evol 3:977-984.

24   Vitti JJ, Grossman SR, Sabeti PC. 2013. Detecting natural selection in genomic data. Annu

25   Rev Genet 47:97-120.

1 Voight BF, Kudaravalli S, Wen X, Pritchard JK. 2006. A map of recent positive selection in

2   the human genome. PLoS Biol 4:e72.

3 Wilde S, Timpson A, Kirsanow K, Kaiser E, Kayser M, Unterlander M, Hollfelder N,

4   Potekhina ID, Schier W, Thomas MG, et al. 2014. Direct evidence for positive selection

5   of skin, hair, and eye pigmentation in Europeans during the last 5,000 y. Proc Natl Acad

6   Sci U S A 111:4832-4837.

7 Williamson SH, Hubisz MJ, Clark AG, Payseur BA, Bustamante CD, Nielsen R. 2007.

8   Localizing recent adaptive evolution in the human genome. Plos Genetics 3:e90.

9 Yi X, Liang Y, Huerta-Sanchez E, Jin X, Cuo ZX, Pool JE, Xu X, Jiang H, Vinckenbosch N,

10   Korneliussen TS, et al. 2010. Sequencing of 50 human exomes reveals adaptation to

11   high altitude. Science 329:75-78.

12 Zeng K, Fu YX, Shi S, Wu CI. 2006. Statistical tests for detecting positive selection by

13   utilizing high-frequency variants. Genetics 174:1431-1439.

14

15

16

1   **Legends**

2   **Fig. 1. Odds ratio for selection mirror the number of selective sweeps in simulated**

3   **populations**

4   Relationship between the odds ratio for selection (OR) and the number of selective sweeps, in

5   computer simulations of African, European and Asian populations, using various numbers of

6   sweeps, $X = [0, 50, 100, 150]$ (1,000 simulated WGSs for each). Simulated PSVs are

7   randomly defined and cover 70% of the genome, a value corresponding to the percent of

8   PSVs defined in the 1000G population. The X selective sweeps were simulated in the African,

9   European or an Asian population, using the two other populations as neutral reference for

10 interpopulation statistics. Each selective sweep has been simulated by considering frequency

11 at the onset of selection varying from $1/2N$ to 0.2 and randomly drawn from the allele

12 frequency spectrum at the onset of selection. For each selective sweep the intensity and the

13 age of selection were randomly drawn from uniform distributions, $s \sim U(0.001, 0.05)$ and

14 $t \sim U(0, 100) \, kya$. We excluded complete sweeps by only keeping simulated sweeps with

15 current selected allele frequencies ranged from 0.2 to 0.95. (**A**) Distributions of the s (left

16 hand side) and t (right hand side) used to simulate the X incomplete sweeps in the African

17 (yellow), European (blue) and Asian (green) population. The initial uniform distributions are

18 indicated in black. (**B**) Simulated ORs for Fay & Wu's H (F&W-H), iHS, DIND, ΔiHH (D-

19 iHH) and two pairwise XP-EHH. The average of the simulated OR are reported within each

20 violin plot.

21

22 **Fig. 2. Accuracy of the ABC estimation of the numbers of selective sweeps**

23 The estimations were performed using the six ORs shown in Fig. 1 and 10^5 ABC simulations

24 obtained similarly as in Fig. 1 but using X randomly drawn in flat prior distributions,

25 $X \sim U(0, 200)$. The priors used for s and t are shown in Fig. 1A. (**A**) ABC estimations of X

47

1   performed in simulated WGSs used as empirical data containing 0, 50, 100 or 150 selective

2   sweeps (200 simulated WGSs in each case). Horizontal red lines indicate the true simulated

3   values of X. (**B**) Relationships between the ABC estimates (y-axis) and the corresponding

4   parameter values (x-axis) obtained for the number of selective sweeps X, as well as for $X_{\underline{1}}$ and

5   X_2, the numbers of sweeps with very low ($1/2N \leq p_{start} < 0.01$) and low ($0.01 \leq p_{start} < 0.1$)

6   frequencies of the selected allele at the onset of selection. The estimations of X_3 (number of

7   sweeps with intermediate initial frequencies, $0.1 \leq p_{start} < 0.2$) are not shown because simply

8   deduced from the relation, $X = X_1 + X_2 + X_3$. In each case, the 200 simulated WGSs used as

9   empirical data were generated following the same recombination and demographic model and

10   using parameters drawn from the priors used for the estimations (top bar plots). Regression

11   lines (colored lines) between true and estimated values and distributions of estimated

12   parameters (right bar plots) are also indicated in each panel. Some classical accuracy indices

13   are also reported, including the 90% COV (Online Methods). Additional information about the

14   accuracy of the ABC estimations of X, S and T are shown in Supplementary Figs. S3-7 (the

15   estimations of S and T corresponding to the panel **A** can be found in Supplementary Fig. S4).

16

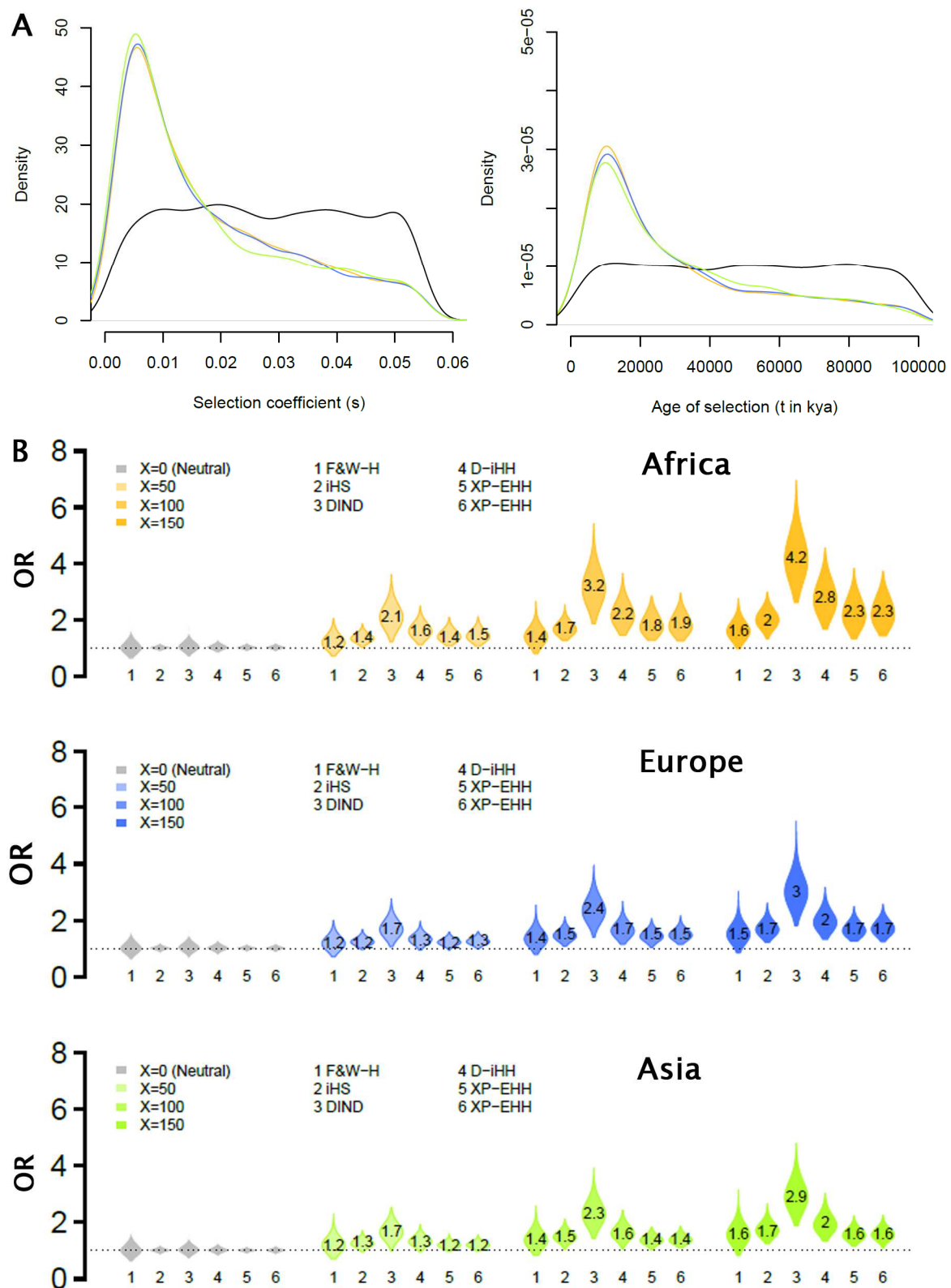17   **Fig. 3. Estimations of the numbers of incomplete selective sweeps**

18   The ABC estimations were performed in each 1000G population separately, using the same

19   summary statistics and ABC simulations as used in Fig. 2B, i.e. six ORs, 10^5 ABC

20   simulations and X randomly drawn in flat prior distributions, $X \sim U(0, 200)$. The priors used

21   for s and t are shown in Fig. 1A. The point estimates and CIs obtained in each population can

22   be found in Supplementary Table S2. Posterior distributions of X in each (**B**) African, (**C**)

23   European and (**D**) Asian population (priors are given in black). Populations used to calibrate

24   the demographic model used (YRI, CEU and CHB) are indicated in bold. (**D**) ABC

25   estimations of X_1, X_2 and X_3, the numbers of selective sweeps with very low

1 (1/2N≤p_{start}<0.01), low (0.01≤p_{start}<0.1) and intermediate (0.1≤p_{start}<0.2) initial frequencies of

2 the selected alleles. (**E,F**) ABC point estimates of the average of the intensity, S, and age of

3 selection, T. The vertical bars shows the minimum and maximum estimates found across all

4 populations considered.

5

6 **Fig. 4. Estimations of the numbers of sweeps including complete selective sweeps**

7 Simulations performed using the same recombination and demographic models used in Figs.

8 1-3 but considering both complete and incomplete selective sweeps (selected allele

9 frequencies ranged from 0.2 to 1). The age of selection t were randomly drawn from uniform

10 distribution, $t \sim U(0, 100)\ kya$. The distribution of the selection coefficient s is an equal mix

11 between a Gamma distribution (60% of s≤0.01) and a L-shape distribution (90% of s≤0.01).

12 (**A**) ABC estimates (y-axis) performed using 2x10^5 ABC simulations using X (x-axis)

13 randomly drawn in flat prior distributions, $X \sim U(0, 300)$. See also the legend of Fig. 2B. (**B**)

14 Simulated ORs obtained for fixed values of X, $X = [100, 150]$, in Europe (blue) and Asia

15 (green). The empirical ORs are indicated in red (solid dots for the populations CEU and

16 CHB). See also the legend of Fig. 1B. Note that the rRMSEs (Online Methods) shown in **A**

17 are higher than assuming incomplete sweeps only (Fig. 2B) because the rate of increase of the

18 OR with X is lower in panel **B** than assuming incomplete sweeps only (Fig. 1B). (**C**) Posterior

19 distributions of X in each European and Asian population (CEU and CHB are indicated in

20 bold). The estimations were performed using 2x10^5 ABC simulations used in **A**. The point

21 estimates and CIs obtained in each population including the African populations, are given in
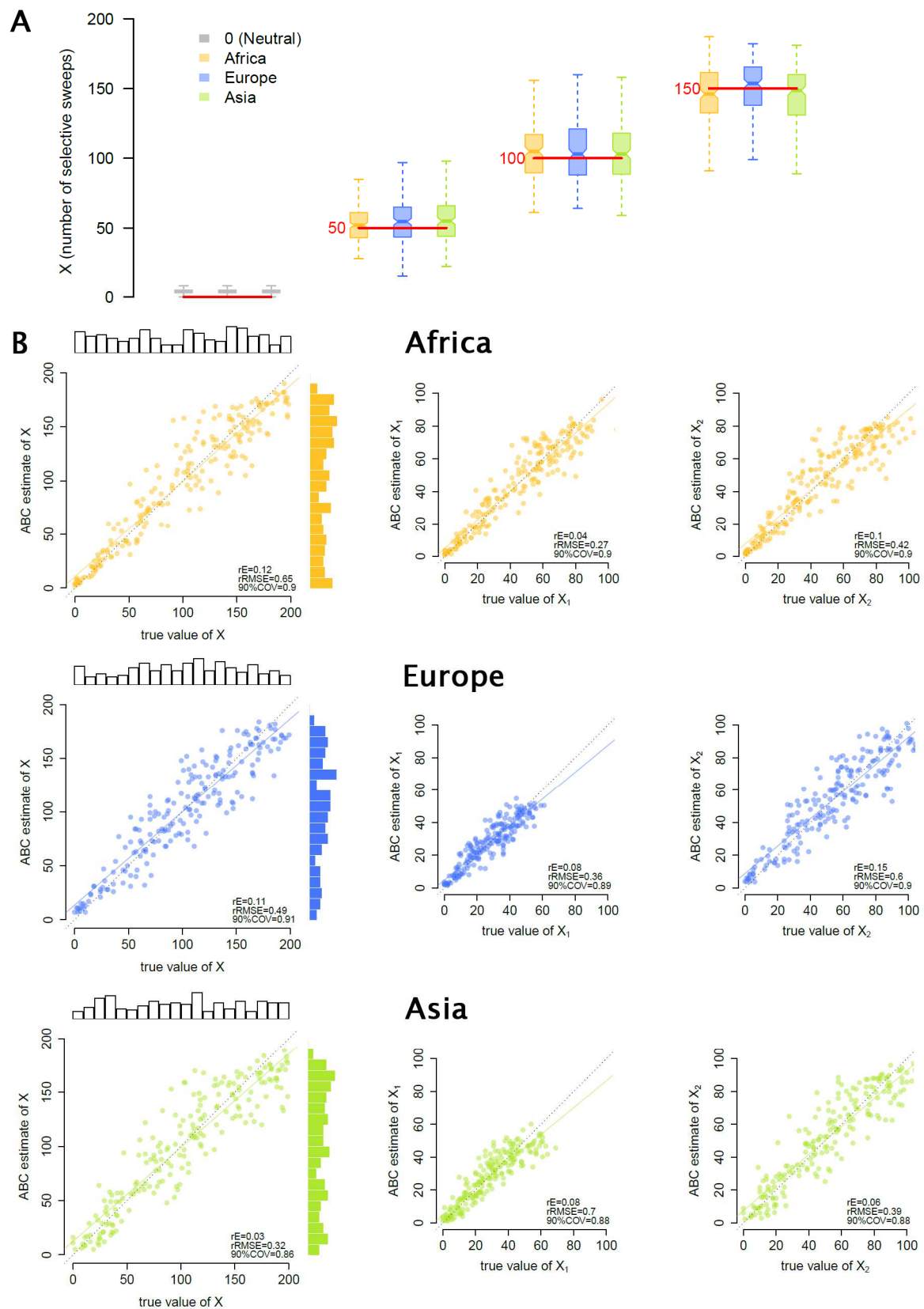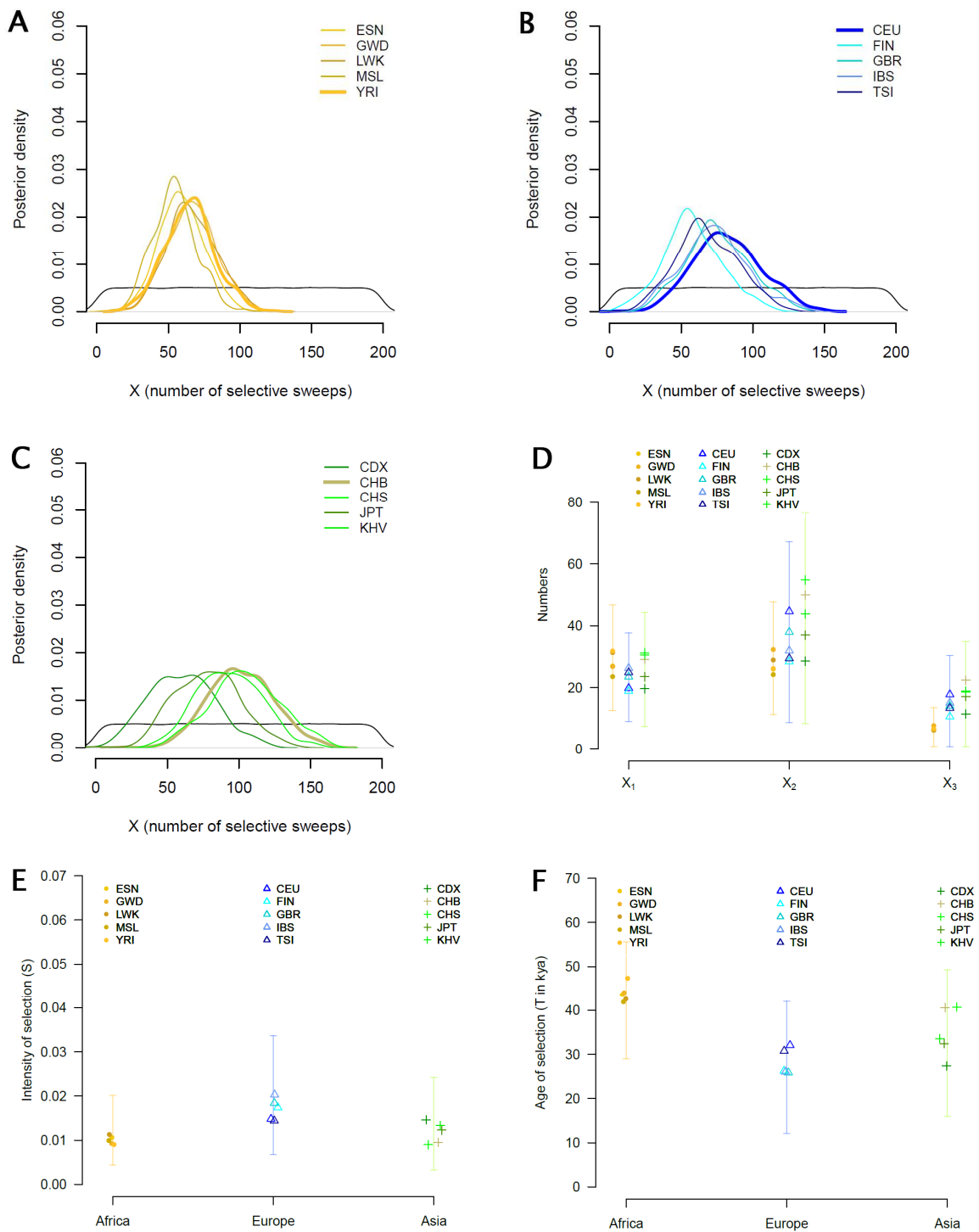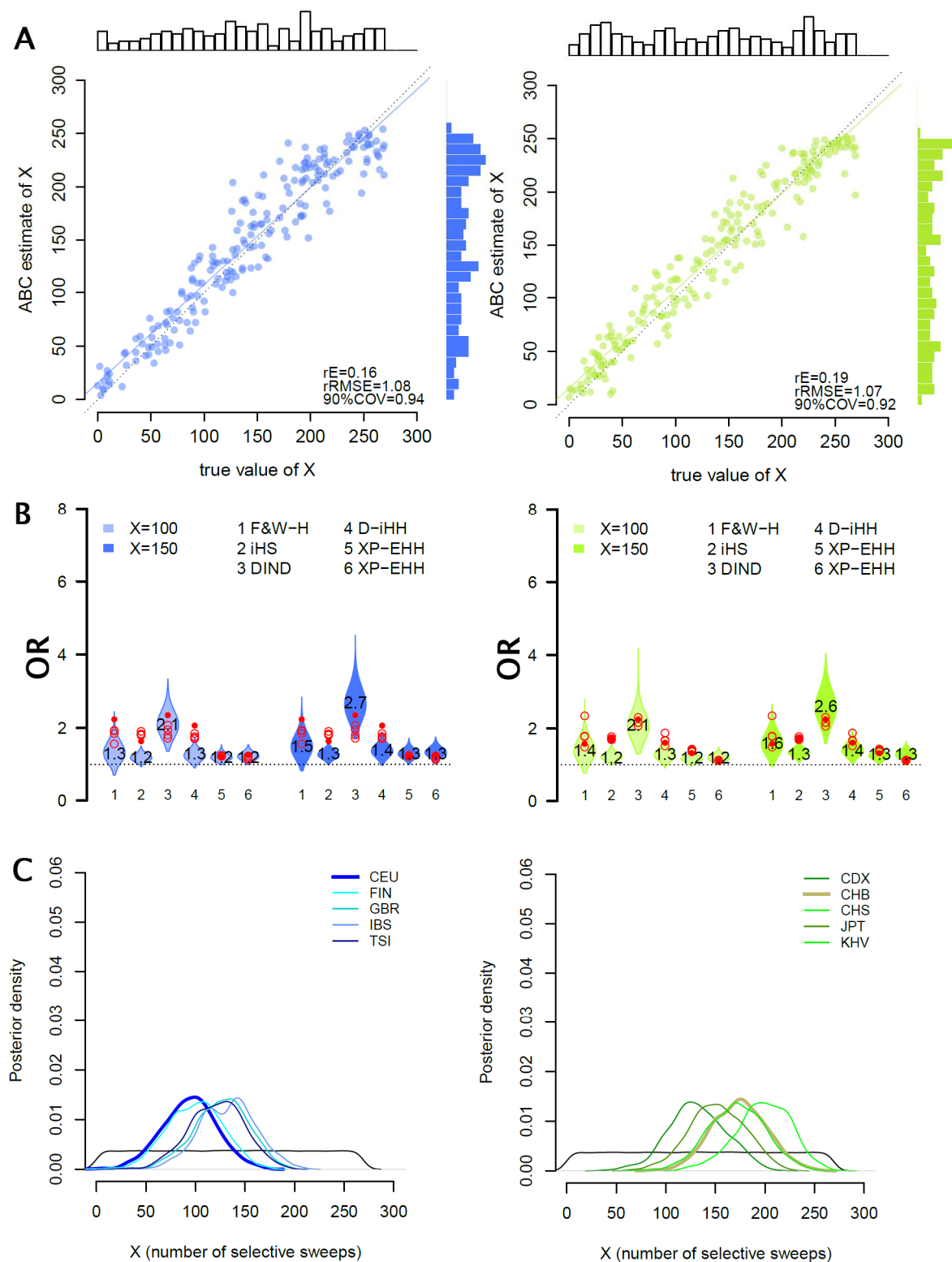
22 Supplementary Table S2.

1   Fig. 1

2

3

1   Fig. 2

2

3

1   Fig. 3

2

3

1   Fig. 4

2

3